protein promoter,[14,15] telomerase promoter,[16] and survivin promoter,[17] have since been made to increase the tumor specificity of CRAd. We showed that CRAd driving an -fetoprotein (AFP) gene promoter had a potent effect on subcutaneous HCC tumors producing AFP in a xenograft model.[9]

However, CRAds in general have the inherent drawback, regardless of their specificity, of relatively low antitumor activity *in vivo*. Thus, relatively large tumors, such as those regularly encountered clinically, may undergo proliferation before the CRAd disseminates throughout the tumor burden. Viral-mediated oncolysis generally requires a latent period during which the viral particles replicate to reach the limiting state and burst the infected cells.

To overcome this drawback, CRAd has been combined with a proapoptotic transgene.[18] However, in most such investigations, the transgenes were integrated in tandem in CRAds.[19-21] In this configuration, it is not possible to adjust the system to achieve either the optimal ratio of viral gene expression to transgene expression or the timely expression of each gene to induce efficient oncolysis. Furthermore, there may be a certain probability of homologous recombination occurring for such CRAds carrying transgenes. In some investigations, the coinfection of a replication-defective adenovirus (RDAd) carrying a proapoptotic gene with CRAd was performed, with the expectation of transactivation of the former virus by early region 1A (E1A) of the latter.[22,23]

In general, investigations that have used the cytocidal approach have found that a greater level of cytotoxicity is attained by coinfection with two different viruses. However, in most instances in which CRAds and RDAd carrying proapoptotic transgenes were coinfected, the viruses were designed to replicate in dividing cells, regardless of their malignant or benign nature. Clearly, tumor specificity is essential to avoid adverse effects.[22]

Another approach designed to overcome the low antitumor activity of CRAds is to combine their use with chemotherapy. Some anticancer drugs including 5-fluorouracil (5-FU), which is often used for the treatment of HCC, are known to enhance viral replication even at subtumoricidal dosages that do not induce any adverse effects.[24-26] This enhancement effect may also be expected to apply to the proapoptotic activity of a transgene product, in particular p53, following stabilization by phosphorylation of Ser20.[27]

In the present study, we designed a CRAd and RDAd p53 gene driven by an AFP promoter. We examined the effect of coinjection of both viruses in combination with the intraperitoneal administration of a subtumoricidal dose of 5-FU on 10-mm-diameter HCC tumors (Hep3B) xenografted into nude mice. Even though the dosages of viruses and 5-FU administered were far lower than those of previous reports,[28-31] we found a remarkable antitumor effect and prolongation of survival in comparison with those found after CRAd, adenoviral p53 (Adp53), or 5-FU was administered individually or in any double combination. Thus, the treatment modality developed here may hold promise for future clinical applications.

Materials and Methods

Cells. The human HCC cell lines Hep3B, HepG2, and PLC/PRF/5 (P5) were obtained from the American Type Culture Collection, and HuH7 was obtained from the Japanese Cancer Research Resource Bank (Tokyo, Japan). The human colon cancer cell line M7609 was kindly provided by M. Koie (Hirosaki University of Medicine, Japan). Normal primary human hepatocytes (Hc) were purchased from the Applied Cell Biology Research Institute (Kirkland, WA). Hep3B, HepG2, and P5 cells were cultured in Dulbecco's modified Eagle's medium (Nissui Pharmaceutical Co., Ltd., Tokyo, Japan) containing 10% heat-inactivated fetal bovine serum (FBS; Flow Laboratories, North Ryde, Australia) and penicillin/streptomycin. HuH7 cells were cultured in Roswell Park Memorial Institute 1640 medium (Nissui Pharmaceutical) containing 10% heat-inactivated FBS (Flow Laboratories) and penicillin/streptomycin. Cell culture was performed at 37°C under 5% CO_2.

Animals. Six-week-old female BALB/cAnNCrj-nu/nu mice were purchased from Charles River Laboratories Japan, Inc. (Yokohama, Japan). All animal studies were conducted in accordance with an animal care protocol that was approved by Sapporo Medical University and conformed to National Institutes of Health guidelines.

AFP Measurement. The cells were plated at a density of 1 10^6 cells per 10-cm dish (Becton Dickinson, NJ) and cultured at 37°C for 24 hours. The culture medium was then replaced by fresh medium containing no FBS. After 2 days of culture, AFP concentrations in the medium were measured with a Hope enzyme-linked immunosorbent assay AFP kit (Hope Laboratories, Belmont, CA).

Doubling Time. Cells were plated in 96-well tissue culture plates (Falcon Labware, Franklin Lakes, NJ) at a density of 2 10^3 cells/cm^2. The following day, the cells were rinsed once and replated with Dulbecco's modified Eagle's medium plus 10% dialyzed FBS, and the medium was changed thereafter every 48 hours. At specific times over 7 days, relative cell numbers per well were determined by the 3-[4,5-dimethylthiazol-2-yl]-2,5-diphenyltetrazolium bromide colorimetric assay (Sigma, St.

Louis, MO) on a plate reader (Anthos Labtec, Frederick, MD) at a wavelength of 550 nm with a 650-nm reference filter. Relative growth rates, as a function of time (days), were determined by graphical evaluations of the optical density.

Construction of Recombinant Adenoviral Vectors. We constructed a selectively replication-competent adenovirus, AdAFPep/Rep, which is driven by -fetoprotein enhancer/promoter (AFPep) with a replication-incompetent adenovirus carrying a p53 transgene that is also driven by AFPep, as described previously.[9,32] Briefly, a pAF5.1–chloramphenicol acetyltransferase plasmid (a kind gift from T. Tamaoki, University of Calgary, Canada), encoding chloramphenicol acetyltransferase under the control of the 5.1-kb 5 -flanking sequence of the AFP gene, was used as a polymerase chain reaction template. The AFP 0.7-kb enhancer and the AFP 0.3-kb promoter were separately amplified with primers that introduced the BglII and BsrGI restriction sites and the BsrGI and HindIII restriction sites, respectively. For the AFP enhancer, we used the sense primer 5 -CAATTAGATCTA-AATTAGTTTTGAATC-3 and the antisense primer 5 -GGCCTGTACAAAGCTGAGTGG-3 ; the Bgl II and BsrGI recognition sites are underlined. For the AFP promoter, we used the sense primer 5 -TATTCTGTACAT-TGAGGAGAATATTG-3 and the antisense primer 5 -GCATGCAGGAAGCTTGTTATTGGC-3 ; the BsrGI and HindIII recognition sites are underlined. To make the adenovirus shuttle vector, the following fragments were cloned into pAd*Bgl*II (kindly provided by M. Imperiale, University of Michigan, MI) as described previously: AFP enhancer, AFP promoter, E1A-13S with a terminal simian vacuolating virus 40 polyadenylation signal, E1B-19K (kindly provided by E. White, Cold Spring Harbor Laboratory, NY) under the control of a cytomegalovirus promoter (CMVp), and bovine growth hormone polyadenylation signal of pRc/cytomegalovirus (Invitrogen). The resulting shuttle vector was designated pAd*Bgl*II-AFPep/E1A13S/CMVp/E1B-19K.

The replication-competent adenovirus, AdAFPep/Rep, expressing E1A-13S driven by -fetoprotein enhancer/promoter (AFPep), was generated by the cotransfection of pAd*Bgl*II-AFPep/E1A-13S/CMVp/E1B-19K and pJM17 (Microbix, Biosystems, Toronto Canada) into HEK293 cells as described previously.[33,34] A replication-deficient adenovirus vector carrying the *Escherichia coli* -galactosidase gene with a nuclear localization signal under the control of AFPep (AdAFPep/nlacZ) and an RDAd carrying the p53 gene under the control of AFPep (AdAFPep/p53) were also generated as described previously.[8] Viral titers were determined by the cytopathic effect assay with HEK293 cells as previously described.[35] Polymerase chain reaction was performed to exclude the possibility of wild-type adenovirus contamination in recombinant AdAFPep/Rep.

Adenoviral Infection. Adenoviral infection was carried out by the simple addition of the virus to the cells (1 10^4) in 24-well plates (Falcon, Becton Dickinson, NJ) at various multiplicities of infection (MOIs) at 37°C in 5% CO_2.

In Vitro *Transduction by AdAFPep/lacZ.* Hep3B cells were plated in 24-well plates at a density of 1 10^4 cells per well and cultured for 24 hours. Immediately before infection, the culture medium was aspirated, and a 50-MOI AdAFPep/lacZ suspension or a 50-MOI AdAFPep/lacZ suspension and a 5-MOI AdAFPep/Rep suspension were added to monolayers. After a 96-hour incubation, -D-galactosidase expression was evaluated with X-gal as the substrate. A blue precipitate in the cell nucleus indicated -D-galactosidase expression.

Immunotransblot Analysis of p53. Hep3B cells were infected with AdAFPep/nlacZ (11 MOI), AdAFPep/Rep (11 MOI), AdAFPep/nlacZ (10 MOI) in combination with AdAFPep/Rep (1 MOI), or AdAFPep/p53 (10 MOI) in combination with AdAFPep/Rep (1 MOI). After 5 days of culture, the Hep3B cells were harvested. After being washed twice with Hank's solution, Hep3B cell pellets from cultures infected with AdAFPep/p53 or AdAFPep/p53 combined with AdAFPep/Rep were suspended in 0.2 mL of a lysis buffer. The protein solutions (10 mg/lane) were loaded onto a 7.5% sodium dodecyl sulfate polyacrylamide gel and electrophoresed; the separated proteins were then electroblotted onto a nitrocellulose membrane. The p53 band was visualized with the mouse monoclonal antibody DO-1 (Santa Cruz Biotechnology, Santa Cruz, CA) against p53 and a sheep anti-mouse secondary antibody conjugated to horseradish peroxidase (Amersham Pharmacia Biotech, United Kingdom).

Immunofluorescent Analysis of p53 and E1A. Hep3B cells infected by AdAFPep/p53 with or without AdAFPep/Rep and cultured in the presence or absence of 5-FU were washed three times with phosphate-buffered saline (PBS), fixed for 1 minute with 50% acetone and 50% methanol, and then washed an additional three times with PBS. For *in vivo* study, the tumors were fixed with formalin and embedded in paraffin, and 10- m sections were cut. Before immunolabeling, a heat-retrieval treatment was conducted. The DO-1, DO-7 (Zymed Laboratories, Carlsbad, CA), or E1A (clone M58, BD Biosciences, Tokyo, Japan) antibody was then applied to the cells or tissue sections and detected with a fluorescein isothiocyanate–conjugated donkey anti-mouse secondary antibody, a fluorescein isothiocyanate–conjugated anti–

immunoglobulin G 2b specific antibody, or a rhodamine-conjugated anti–immunoglobulin G 2a specific antibody (Rockland, Gilbertsville, PA). The cells were viewed and images were obtained with a confocal imaging system (MRC-1024, Bio-Rad). The number of p53-positive cells was counted in each experiment, and the relative expression ratio was calculated as the ratio of the number of p53-positive cells to the number of Hep3B cells infected only with AdAFPep/p53.

Cytotoxicity Assay. Hep3B cells were plated at a density of 1 10^5 cells per well in a 24-well plate, and then the cells were infected with the various adenoviruses described previously. The viability of infected cells, in the presence or absence of anticancer drugs, was determined by an MTT assay.[36,37]

Assaying the Virus Yield. At various times post-infection, the cells were dislodged into the culture medium by scraping, and they were then lysed by three cycles of freezing and thawing. The supernatant or purified virus was tested for viral titer by an endpoint cytopathic assay as described previously.[38] Briefly, 50 L of DMEM with 5% FBS (5% FBS DMEM) was dispensed into each well of a 96-well tissue-culture plate, and then a 3-fold serial dilution of the virus starting from a 10^{-4} dilution was prepared in each well; 3 10^5 of HEK293 cells in 50 L of 5% FBS DMEM was added to each well. The endpoint of the cytopathic effect was determined by microscopy on day 12, and a 50% tissue culture infectious dose was calculated.

Quantitative Analysis of Synergy. The Chou-Talalay multiple drug effect analysis was used to determine the pharmacological interaction between AdAFPep/Rep and AdAFPep/p53. This analysis can be used to determine the extent of synergism or antagonism by a comparison of how much the combination effect differs from the expected additive effect of the two therapeutic agents. The method has been described previously.[39] Such analysis involves plotting dose-effect curves for each therapy and multiplying diluted combinations of the therapies with the median effect equation. A combination index (CI) is then determined. At CI 1, the interaction is considered additive. At CI 1, synergy is indicated, and at CI 1, antagonism is indicated.

In Vivo *Treatment Protocol.* Hep3B cells (1 10^7/mouse) were subcutaneously inoculated into the lateral abdominal walls of 6-week-old female BALB/cAnNCrj-nu/nu mice (n 40), and tumors were allowed to grow to 10 mm in diameter (tumor volume of 500 mm^3). Then, we conducted a single injection of AdAFPep/p53 and AdAFPep/Rep into tumors. Mice were then divided into eight groups (n 5 for each group). The first group was given PBS intratumorally on day 0. The second group was given an intraperitoneal administration of 5-FU (600 g/body) on days 4 to 6, days 11 to 13, days 18 to 20, and days 25 to 27. The remaining six groups received AdAFPep/p53 (2 10^8 pfu/200 L), AdAFPep/Rep (0.2 10^8 pfu/20 L), or AdAFPep/p53 plus AdAFPep/Rep (0.2 10^8 pfu) on day 0 with or without intraperitoneal administration of 5-FU on days 4 to 6, days 11 to 13, days 18 to 20, and days 25 to 27. Each mouse was administered a total viral dosage of 2.2 10^8 pfu (shown later in Fig. 8A,B). The intratumoral injection was performed at four separate places of the tumor to attain efficient infection of adenovirus vectors. Next, we conducted multiple injections of AdAFPep/p53 and AdAFPep/Rep into tumors. Mice were injected with AdAFPep/p53 and AdAFPep/Rep on 7 consecutive days. The administering schedule of 5-FU was the same as previously described.

Tumor diameters were measured with calipers, and tumor volumes were calculated by the formula $(aT)^2$ (bT)/2, where (aT) represents the shortest diameter and (bT) represents the longest distance. All tumor-bearing mice were sacrificed when the tumor size reached 2000 mm^3 in accordance with the ethical guidelines of the Sapporo Medical University animal committee in order to prevent the mice from suffering from a large tumor burden.

Immunohistochemical Analysis of CD34 and Brain-Specific Angiogenesis Inhibitor 1 (BAI-1). Tumors were resected on day 5 after treatment of adenoviral vectors and/or 5-FU. The expression of CD34 and p53-target gene BAI-1 was evaluated by immunohistochemical staining. Formalin-fixed, paraffin-embedded tissues were immunostained with the monoclonal antibody to CD34 (Dako, Carpinteria, CA), BAI-1 (MBL International Corp., Medical and Biological Laboratories, Japan), and biotin-labeled anti-mouse immunoglobulin G and horseradish peroxidase–conjugated streptavidin (Nichirei, Japan) according to the manufacturer's instructions (Dako).

Results

AFP Production and Doubling Time of Human HCC Cells. First, we assayed the culture supernatants of the HCC cell lines for AFP production by enzyme-linked immunosorbent assay. AFP was detected in the culture media of the Hep3B, P5, HuH7, and HepG2 cell lines with concentrations ranging from 5.2 to 12,970 ng/day/10^6 cells. P5, Hep3B, HuH7, and HepG2 produced AFP in the culture media at concentrations of 73 6, 5.2 0.8, 12,970 1067, and 633 23 ng/day/10^6 cells. AFP was undetectable in the media of Hc and the human colon cancer cell line M7609. The proliferation rates of the

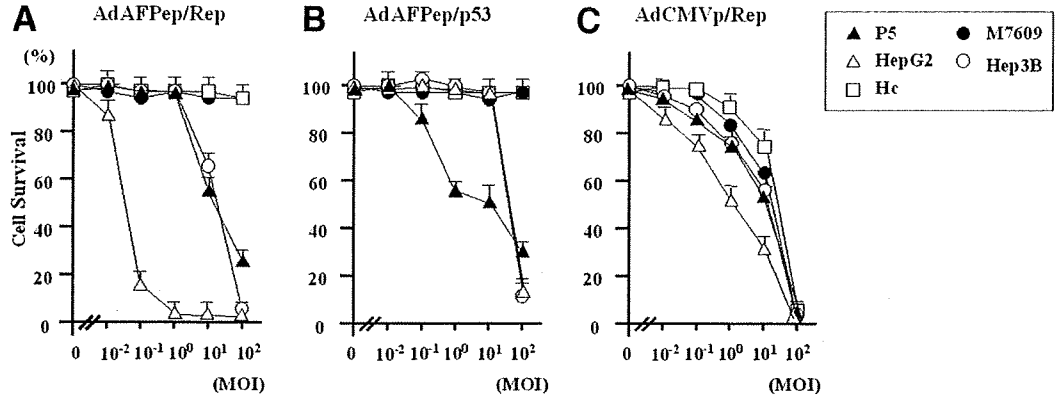

Fig. 1. Specificity of AdAFPep/Rep and AdAFPep/p53 to -fetoprotein-producing cells. Four cancer cell types (Hep3B, HepG2, PLC/PRF/5, and M7609) and a normal cell type (Hc) were infected with (A) AdAFPep/Rep, (B) AdAFPep/p53, or (C) AdCMVp/Rep at various MOIs. Cytotoxicity was measured by an MTT assay at day 7 post-infection. The data are the means standard deviation (bars) of a representative experiment performed in triplicate. Abbreviations: Hc, primary human hepatocytes; MOI, multiplicity of infection.

HCC cell lines were measured with doubling times. The doubling times of Hc, P5, Hep3B, HuH7, and HepG2 cells were 25 2.3, 40 4.0, 24 3.6, 51 4.1, and 29 4.0 hours, and Hep3B was found to be the most rapidly proliferating cell line. We therefore chose this cell line for subsequent experiments.

Specificity of AdAFPep/Rep and AdAFPep/p53 for AFP-Expressing HCC Cells. To verify the selective toxicity of AdAFPep/Rep and AdAFPep/p53 for AFP-producing cells, we measured the survival of the Hep3B, HepG2, P5, Hc, and M7609 cells after viral infection. Cytotoxicity was measured by an MTT assay at day 7 of infection. The AFP-producing cell lines Hep3B, HepG2, and P5 showed an apparent susceptibility to AdAFPep/Rep and AdAFPep/p53, but the cell types that did not produce AFP, Hc and M7609, were not lysed even at high concentrations of the viruses (up to 100 MOI; Fig. 1A,B). In contrast, all five cell types were lysed by AdCMVp/Rep (Fig. 1C).

Augmentation of nlacZ Expression and p53 Expression in Hep3B Cells Infected with AFPep-Driven RDAd Carrying nlacZ and p53, Respectively, by Combination with AdAFPep/Rep. We sought to validate our expectation that E1A of AdAFPep/Rep would induce transcomplementary activation of RDAd carrying a transgene, as shown in Fig. 2A. First, we examined nlacZ expression in Hep3B cells coinfected with 50-MOI AdAFPep/nlacZ and 5-MOI AdAFPep/Rep and compared this level of expression with that in Hep3B cells infected with 50-MOI AdAFPep/nlacZ only. The experimental concentrations used here for AdAFPep/nlacZ and AdAFPep/Rep were based first on previous reports in which 30 to 50 MOI were used for nlacZ transfection[40,41] and expression experiments and second on the fact that evidence in the present study indicated that a 10:1 ratio of AdAFPep/nlacZ to AdAFPep/Rep was most appropriate for increasing transgene expression (shown later in Fig. 6). Four days after infection, X-gal staining showed a clear increase in nlacZ-positive cells following coinfection with

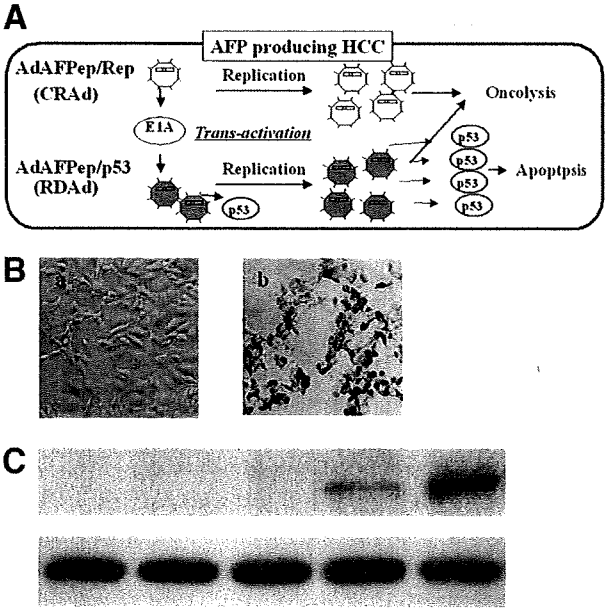

Fig. 2. Enhancement of reporter gene or p53 gene expression in AdAFPep/nlacZ-infected or AdAFPep/p53-infected Hep3B cells by AdAFPep/Rep. (A) Transactivation of AdAFPep/p53 by E1A derived from the replication competent adenovirus AdAFPep/Rep. (B) -Galactosidase staining of Hep3B cells infected with the following CRAds: (a) AdAFPep/nlacZ (50 MOI) and (b) AdAFPep/nlacZ (50 MOI) plus AdAFPep/Rep (5 MOI). (C) Western blot analysis of p53 protein in Hep3B. The lanes show the results of cell homogenates from the following sources: lane 1, no treatment; lane 2, AdAFPep/Rep; lane 3, AdAFPep/nlacZ plus AdAFPep/Rep; lane 4, AdAFPep/p53; and lane 5, AdAFPep/p53 plus AdAFPep/Rep. Abbreviations: AFP, -fetoprotein; CRAd, conditionally replicable adenovirus; E1A, early region 1A; HCC, hepatocellular carcinoma; MOI, multiplicity of infection; RDAd, replication-defective adenovirus.

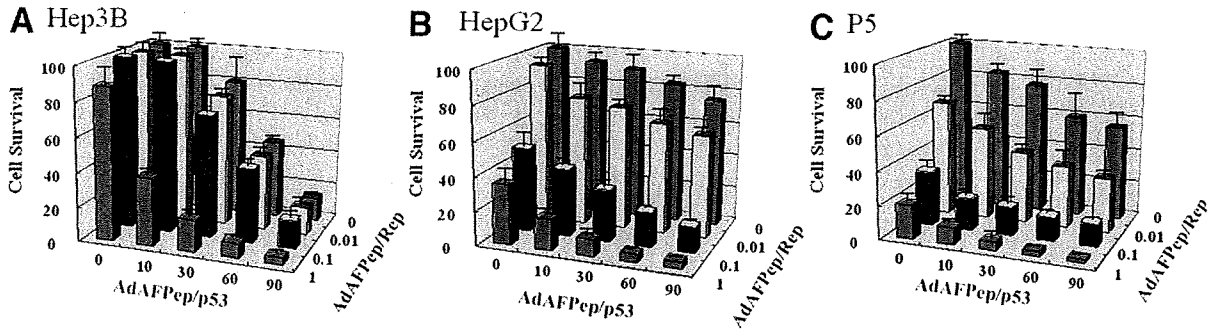

Fig. 3. Synergistic cytotoxicity of AdAFPep/Rep and AdAFPep/p53 in hepatocellular carcinoma cell lines. (A) Hep3B, (B) HepG2, and (C) P5 were infected with AdAFPep/Rep or AdAFPep/p53 at various multiplicities of infection. Cytotoxicity was measured by an MTT assay on day 5 post-infection. The data are the means standard deviation (bars) of a representative experiment performed in triplicate. Abbreviation: P5, PLC/PRF/5.

AdAFPep/nlacZ and AdAFPep/Rep in comparison with infection with AdAFPep/nlacZ alone (Fig. 2B). Transactivation was further examined by western blotting for p53 (Fig. 2C). On day 4 of infection, the intensity of the immunoreactive 53-kDa band in cells infected with AdAFPep/p53 and AdAFPep/Rep was appreciably greater than that in cells infected with AdAFPep/p53 alone. Cells infected with either AdAFPep/Rep alone or AdAFPep/Rep plus AdAFPep/lacZ showed no positive bands.

Synergistic Effect of Combining AdAFPep/Rep and AdAFPep/p53 on Cytotoxicity. The combination of AdAFPep/p53 (10-90 MOI) with AdAFPep/Rep (0.01-1 MOI) appeared to increase cytotoxicity in Hep3B cells, regardless of the ratio of the viruses (Fig. 3A). We performed a Chou-Talalay analysis to examine the synergy of the combined virus treatment in the Hep3B cell line. As shown in Table 1, the assay for cell survival on day 5 of infection, when the effect of cytotoxicity started to be clear, demonstrated that the CI values of all possible combinations of AdAFPep/p53 and AdAFPep/Rep were lower than 1.0, indicating that all combinations displayed synergy. In particular, the CI of the 1:10 ratio of AdAFPep/Rep to AdAFPep/p53 was smallest at 0.25; therefore, this combination was considered to exert the strongest synergistic effect for cytotoxicity in the Hep3B cell line. We further examined whether a similar effect could be observed in other HCC cell lines such as HepG2 and P5. As expected, the combination of AdAFPep/p53 (10-90 MOI) with AdAFPep/Rep (0.01-1 MOI) appeared to increase cytotoxicity in both HepG2 and P5 cell lines (Fig. 3B,C).

Timing of Cotransfection. AdAFPep/p53 was added to Hep3B cells at various intervals after the cells had been infected with AdAFPep/Rep to examine the optimal application time for each virus. Hep3B cells were infected with 1.0-MOI AdAFPep/Rep in combination with AdAFPep/p53 at various concentrations (Fig. 4A, 10 MOI; Fig. 4B, 30 MOI; and Fig. 4C, 60 MOI). Cell survival was measured by an MTT assay 5 days post-infection. We did not find a significant difference in the tumoricidal effect when the viruses were applied together (0 hours) or with a time lag (1, 4, or 24 hours; Fig. 4A). In addition, there was no significant difference in the tumoricidal effect at the various MOI ratios (Fig. 4A-C). Accordingly, in all subsequent experiments, the viruses were applied simultaneously to the Hep3B cells or tumor.

Facilitating Effect of 5-FU on Adenovirus Release from Its Infected Hep3B. We investigated the effect of a subtumoricidal dose of 5-FU on the replication and release of adenoviruses from Hep3B cells infected either with AdAFPep/p53 and AdAFPep/Rep or with AdAFPep/Rep alone. On the basis of a previous report showing that a 4 M (approximately 0.5 g/mL) 5-FU treatment facilitated the replication of an adenovirus,[26] we selected

Table 1. Chou-Talalay Analysis of the Combination Index for 16 Combination Treatments

AdAFPep/p53 (MOI)	AdAFPep/Rep (MOI)	Cell Survival Rate	Combination Index
10	0	0.99	2.684
10	0.0.1	0.31	0.779
10	0.1	0.25	0.500
10	1	0.02	0.250
30	0	0.56	1.014
30	0.01	0.18	0.864
30	0.1	0.16	0.462
30	1	0.02	0.485
60	0	0.26	1.104
60	0.01	0.08	0.927
60	0.1	0.04	0.581
60	1	0.01	0.626
90	0	0.16	1.280
90	0.01	0.04	1.037
90	0.1	0.04	0.822
90	1	0.01	0.658

Abbreviation: MOI, multiplicity of infection.

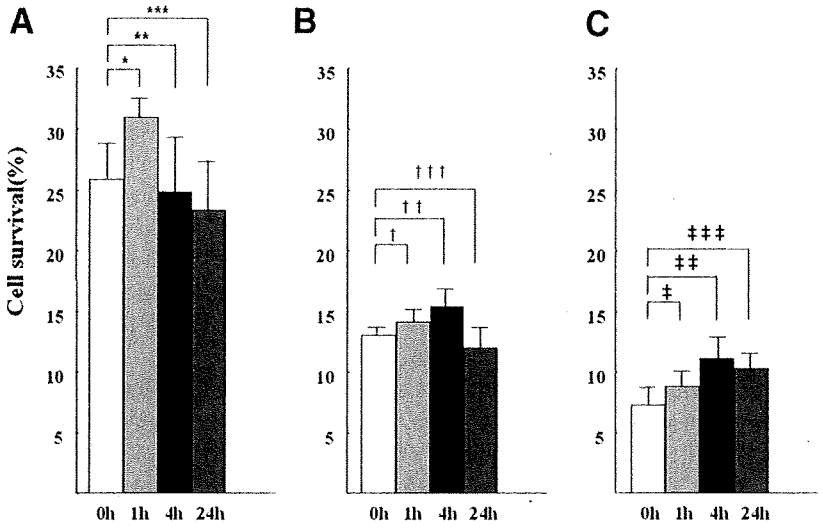

Fig. 4. Effect of infection intervals of AdAFPep/Rep and AdAFPep/p53 on cytotoxicity in Hep3B cells: (A) AdAFPep/Rep (1 MOI) plus AdAFPep/p53 (10 MOI), (B) AdAFPep/Rep (1 MOI) plus AdAFPep/p53 (30 MOI), and (C) AdAFPep/Rep (1 MOI) plus AdAFPep/p53 (60 MOI). AdAFPep/p53 was added to Hep3B cells at various MOIs and at various intervals after the cells had been infected with 1-MOI AdAFPep/Rep. Cytotoxicity was measured by an MTT assay on day 5 post-infection. The results of statistical analysis were as follows: (A) *P 0.110, **P 0.740, and ***P 0.463; (B) †P 0.086, ††P 0.272, and †††P 0.449; and (C) ‡P 0.165, ‡‡P 0.096, and ‡‡‡P 0.109. Abbreviation: MOI, multiplicity of infection.

the dose of 0.5 g/mL 5-FU in this study. On day 5 after the initial infection, 0.5 g/mL 5-FU was added to the culture medium, which by itself did not show any antiproliferative activity (shown later in Fig. 7). Viral concentrations in the culture supernatants were measured by a cytopathic assay on days 5, 7, and 10 after viral infection. The HepB3 cells were infected with relatively low doses of viruses, 10-MOI AdAFPep/p53 and 1.0-MOI AdAFPep/Rep, because of the concern that higher doses might cause rapid tumor cell lysis that might obscure any differences in viral release from tumor cells after different treatments. On day 3 after the infection, viral concentrations in the culture supernatants remained under the detection level. As shown in Fig. 5, viral release was clearly increased 2 days after treatment with 5-FU in comparison with cultures that did not receive the drug, and this clear difference was maintained in the 10-day sampling interval. Incidentally, we evaluated lower and higher doses of 5-FU. A 0.05 g/mL 5-FU treatment showed no effect on the replication of the adenovirus; conversely, 5 g/mL 5-FU induced tumor cell lysis before the replication of the adenovirus.

5-FU Augments p53 Expression in Hep3B Cells Infected with AdAFPep/Rep and AdAFPep/p53. Cellular stresses, including exposure to anticancer drugs, induce p53 expression. We therefore examined the effect of 5-FU on p53 expression in Hep3B cells infected with 10-MOI AdAFPep/p53 with or without 1-MOI AdAFPep/Rep. The cells were incubated with the viruses for 5 days and for another 3 days in the presence of 0.5 g/mL 5-FU. The rate of p53-positive cells increased slightly but significantly (7-fold) in cultures infected with AdAFPep/p53 and exposed to 5-FU (Fig. 6B) in comparison with those with AdAFPep/p53 alone.

The immunofluorescence intensity of Hep3B cells coinfected with AdAFPep/p53 and AdAFPep/Rep was substantially increased (approximately 170-fold) in comparison with that of cells treated with AdAFPep/p53 alone, reflecting the synergistic effect of coinfection. This increase was augmented approximately 2.2-fold by the addition of 5-FU.

5-FU Augments Cytotoxicity in Cells Infected with AdAFPep/Rep and AdAFPep/p53. We next investigated the effect of 5-FU on cytotoxicity in cells coinfected with 10-MOI AdAFPep/p53 and 1.0-MOI AdAFPep/Rep. Hep3B cells that had been infected with both viruses were cultured for 5 days, and then 0.5 g/mL 5-FU was

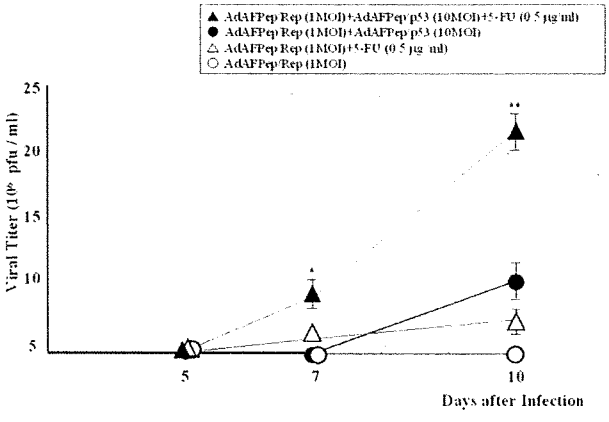

Fig. 5. Effect of 5-FU on the release of adenoviruses from Hep3B cells infected with AdAFPep/p53 and AdAFPep/Rep: (▲) AdAFPep/Rep (1 MOI) plus AdAFPep/p53 (10 MOI) plus 5-FU (0.5 g/mL), (●) AdAFPep/Rep (1 MOI) plus AdAFPep/p53 (10 MOI), (△) AdAFPep/Rep (1 MOI) plus 5-FU (0.5 g/mL), and (○) AdAFPep/Rep (1 MOI). Hep3B cells were infected with 10-MOI AdAFPep/p53 and 1-MOI AdAFPep/Rep. The cells and supernatant were harvested on days 3, 5, 7, and 10 after infection, and the virus yield was measured by titration on 293 cells. *P 0.05, closed triangles versus closed circles. **P 0.01, closed triangles versus closed circles (Student t test). Abbreviations: 5-FU, 5-fluorouracil; MOI, multiplicity of infection.

added to the culture medium. Cell survival was determined by an MTT assay on days 3, 5, 7, 10, and 13 after the initiation of the culture (Fig. 7). Those cells treated with AdAFPep/lacZ alone, with AdAFPep/p53 alone, with 5-FU alone, or with AdAFPep/p53 plus 5-FU showed growth curves similar to that of nontreated cells during the observation period. The growth of AdAFPep/Rep-infected cells was somewhat but significantly impaired in comparison with that of nontreated cells. More marked growth suppression was observed in cells treated with both AdAFPep/Rep and AdAFPep/p53. The addition of subtumoricidal-dose 5-FU clearly and significantly augmented growth suppression effects of both AdAFPep/Rep alone and AdAFPep/Rep with AdAFPep/p53 in combination.

In Vivo Antitumor Effect of 5-FU in Combination with AdAFPep/Rep and AdAFPep/p53. The *in vitro* experiments described previously indicated that 5-FU in combination with coinfection by AdAFPep/Rep and AdAFPep/p53 reduced the ability of Hep3B cells to proliferate. Our next step was therefore to determine whether this combination was also effective *in vivo*. Nude mice (n 40) were given a subcutaneous dorsal inoculation of 1 10^7 Hep3B cells. When tumors were established and reached 10 mm in diameter, they were injected with either PBS or 2 10^8 pfu AdAFPep/p53 and 0.2 10^8 pfu AdAFPep/Rep on day 0, and 5-FU was administered on 3 consecutive days. Tumors injected with AdAFPep/p53 grew at almost the same rate as those injected with PBS (Fig. 8A). However, the injection of AdAFPep/Rep significantly suppressed tumor growth in comparison with the PBS group. A statistically significant suppression of tumor growth resulted from the injection of a combination of AdAFPep/p53 and AdAFPep/Rep in comparison with the group that received AdAFPep/Rep alone. Treating the tumors with 5-FU augmented the growth suppression effects of the various treatments described. The most significant effect was observed with the combination of AdAFPep/p53, AdAFPep/Rep, and 5-FU (Fig. 8A).

For ethical reasons, the mice were sacrificed before the xenografted tumor grew to a volume of 2000 mm^3. Therefore, the true survival curve of each group of mice was not obtained. However, it is clear from Fig. 8B that mice given a combination of AdAFPep/Rep and AdAFPep/p53 with 5-FU showed the longest survival.

We next examined whether repeated daily coinjections of AdAFPep/p53 and AdAFPep/Rep would ameliorate the efficacy. As expected, after seven coinjections, the tumor completely disappeared and never recurred for at least 40 days (during the observation period; Fig. 8C). However, in the other control group, complete regression was not observed

Validation of Coinfection of AdAFPep/p53 and AdAFPep/Rep. To validate coinfection in a single cell, *in vivo* immunofluorescence analysis was performed. The existence of each adenovirus was assessed with anti-p53 and anti-E1A antibodies. As shown in Fig. 9, AdAFPep/p53-infected cells were observed as a green color, and AdAFPep/Rep-infected cells were detected as a red color. Importantly, several cells were proven to be coinfected (yellow color in the overlay panel), and this indicated that coinfection actually occurred after the injection of both adenoviruses *in vivo*.

In Vivo *Angiogenetic Effects of AdAFPep/Rep, AdAFPep/p53, and 5-FU.* To evaluate the antiangiogenic effects of a combination of AdAFPep/Rep, AdAFPep/p53, and 5-FU in xenografted tumors, immunohistochemical staining was performed. Multiple CD34 endothelial cells were detected in xenografted HCC tumors in nontreated nude mice. In clear contrast, no CD34 endothelial cells were observed in HCC tumors in nude mice treated with AdAFPep/Rep, AdAFPep/p53, and 5-FU (Fig. 10A). Moreover, the expression of the antiangiogenic factor BAI-1, which is a direct target gene of p53, was enhanced in xenografted HCC tumors with AdAFPep/Rep, AdAFPep/p53, and 5-FU (Fig. 10B), and this suggested that an antiangiogenic effect could also contribute to inhibition of tumor growth in a combination therapy of AdAFPep/Rep, AdAFPep/p53, and 5-FU *in vivo*.

Discussion

In the present study, we aimed to overcome the relatively low antitumor activity of CRAd, which is a drawback to its use as a therapy for hepatic cancer. Our experiments have demonstrated that the combination of CRAd with AdAFPep/p53 and low-dose 5-FU shows promise for such therapy. We successfully achieved prolonged suppression of relatively large HCC tumors (10 mm in diameter) in nude mice by a single injection of the two viruses followed by maintenance administration of 5-FU.

We paid particular attention to two technical issues in our development of this approach: the tumor specificity of the viruses and the timing of the administration of each virus. As we wish ultimately to develop a therapy for use with HCC, we employed the AFP promoter here, which we constructed previously, with both viruses to ensure the specific replication of CRAd and the specific expression of p53 in AFP-producing cells, although this approach may not be applicable for highly differentiated HCCs, which often are negative for AFP. Our results confirmed the success of this approach (Fig. 1). Tumor specificity was a critical issue for our strategy in order to prevent damage to normal proliferating cells since the cytocidal effect of

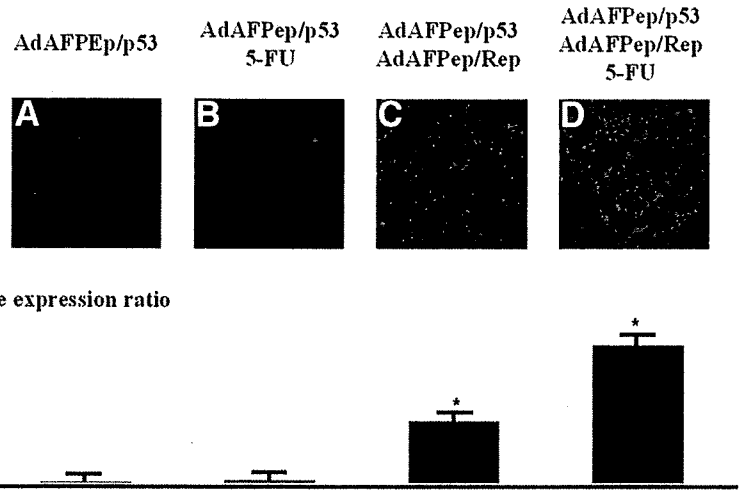

Fig. 6. Effect of 5-FU on p53 expression in Hep3B cells infected with AdAFPep/p53 and AdAFPep/Rep: (A) AdAFPep/p53 (10 MOI), (B) AdAFPep/p53 (10 MOI) plus 5-FU (0.5 g/mL), (C) AdAFPep/p53 (10 MOI) plus AdAFPep/Rep (1 MOI), and (D) AdAFPep/p53 (10 MOI) plus AdAFPep/Rep (1 MOI) plus 5-FU (0.5 g/mL). Hep3B cells were infected with 10-MOI AdAFPep/p53 with or without 1-MOI AdAFPep/Rep. After incubation for 5 days, 0.5 g of 5-FU was added, and the cells were incubated another 3 days. p53 expression was detected by an immunofluorescence method. *P 0.01, AdAFPEp/p53 versus AdAFPep/p53 plus AdAFPep/Rep plus 5-FU (Student t test). Abbreviations: 5-FU, 5-fluorouracil; MOI, multiplicity of infection.

AdAFPep/Rep was enhanced considerably by the use of AdAFPep/p53 and 5-FU.

Although the AFP promoter functioned well in AFP-producing HCC cells, one concern is that it might also activate viruses in the AFP-producing hepatocytes often seen in livers affected by hepatitis. However, because our AdAFPep/Rep has a deletion of E1B-55k, it will not replicate in hepatocytes that produce wild-type p53. Therefore, our AdAFPep/Rep is endowed with a double assurance for specificity by the AFPep and the E1B-55k deletion. Collectively, our proposed therapy would be primarily applied to advanced stages of HCC because p53 mutation is a late molecular event in most HCC development.

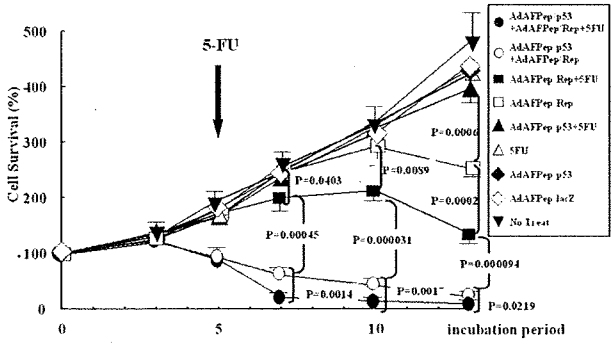

Fig. 7. Effect of 5-FU on the cytotoxic effect of AdAFPep/Rep in combination with AdAFPep/p53: ( ) no treatment, ( ) AdAFPep/lacZ (10 MOI), ( ) AdAFPep/p53 (10 MOI), (△) 5-FU (0.5 g/mL), (▲) AdAFPep/p53 (10 MOI) plus 5-FU (0.5 g/mL), ( ) AdAFPep/Rep (1 MOI), ( ) AdAFPep/Rep (1 MOI) plus 5-FU (0.5 g/mL), (○) AdAFPep/p53 (10 MOI) plus AdAFPep/Rep (1 MOI), and (●) AdAFPep/p53 (10 MOI) plus AdAFPep/Rep (1 MOI) plus 5-FU (0.5 g/mL). Hep3B cells were infected with 10-MOI AdAFPep/p53 and 1.0-MOI AdAFPep/Rep. Five days after coinfection, 0.5 g of 5-FU was added. Cytotoxicity was determined by an MTT assay on days 3, 5, 7, 10, and 13 after initiation of the culture. Abbreviations: 5-FU, 5-fluorouracil; MOI, multiplicity of infection.

Identification of the optimal administration schedule for each virus was also important for efficient transactivation of the RDAd-carrying transgene by CRAd. Transactivation might require an appropriate time lag between E1A expression by CRAd and expression of the transactivated RDAd genes. Furthermore, overexpression of the p53 transgene due to inappropriate timing might result in cell cycle arrest, which would hamper the replication efficiency of CRAd. These concerns were proved groundless in our investigation as our results indicated that the time lag between the administration of each virus was irrelevant to the cytolytic efficacy. We therefore chose the simultaneous application protocol for the *in vivo* treatment (Fig. 8A). The reason that the timing of administration of the viruses is irrelevant is unclear at present. Very low levels of E1A expression were present soon after CRAd infection, and these might be adequate for adenovirus production. If so, then this might explain why the cytolytic activity of simultaneously administered viruses is similar to that of viruses administered with a time lag.

It has been reported that tumors considerably smaller than 10 mm in diameter can be treated with a single administration of a cytotoxic gene, an oncolytic virus, or a combination of the two. Here we injected one-fifth of the amount of AdAFPep/Rep (0.2 10^8 pfu) used to successfully eradicate small tumors of 100 mm^3 (0.2 10^8 pfu). Additionally, the amount of AdAFPep/p53 administered *in vivo* in our study was also approximately one-fifth to one-thirtieth of those used previously for *in vivo* tumor treatments. Our strategy proved to be quite effective for suppressing the growth of tumors as large as 500 mm^3, the size that might be encountered clinically. With

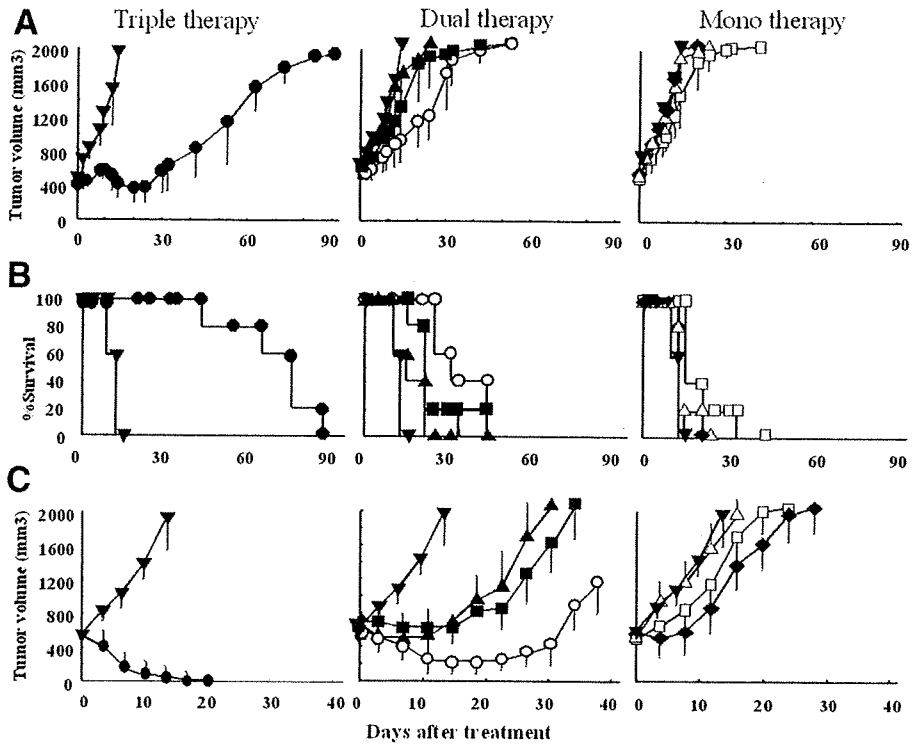

Fig. 8. (A) *In vivo* antitumor effect of a single injection of AdAFPep/Rep, AdAFPep/p53, and 5-FU in combination: ( ) PBS, ( ) AdAFPep/p53, (△) 5-FU, (▲) AdAFPep/p53 plus 5-FU, ( ) AdAFPep/Rep, ( ) AdAFPep/Rep plus 5-FU, (○) AdAFPep/p53 plus AdAFPep/Rep, and (●) AdAFPep/p53 plus AdAFPep/Rep plus 5-FU. Hep3B cells (1 10^7) were inoculated subcutaneously into the backs of nude mice, and either 220 L of PBS or 2.2 10^8 pfu/220 L of viruses was injected into established tumors when they had grown to 10 mm in diameter. Each experimental group contained five mice. Intratumoral injection of AdAFPep/Rep and AdAFPep/p53 suppressed tumor growth. In addition, treatment of the mice with 5-FU augmented the effect of the viruses. Tumor diameters were measured with calipers, and tumor volumes were calculated as described in the Materials and Methods section. (B) Survival of mice after treatment with AdAFPep/Rep in combination with AdAFPep/p53 and 5-FU: ( ) PBS, ( ) AdAFPep/p53, (△) 5-FU, (▲) AdAFPep/p53 plus 5-FU, ( ) AdAFPep/Rep, ( ) AdAFPep/Rep plus 5-FU, (○) AdAFPep/p53 plus AdAFPep/Rep, and (●) AdAFPep/p53 plus AdAFPep/Rep plus 5-FU. A survival curve for the mice of each treatment group (n 5) is shown. Mice treated with AdAFPep/Rep in combination with AdAFPep/p53 and 5-FU showed a significantly higher survival rate. (C) *In vivo* antitumor effect of multiple injections of AdAFPep/Rep, AdAFPep/p53 and 5-FU in combination: ( ) PBS, ( ) AdAFPep/p53, (△) 5-FU, (▲) AdAFPep/p53 plus 5-FU, ( ) AdAFPep/Rep, ( ) AdAFPep/Rep plus 5-FU, (○) AdAFPep/p53 plus AdAFPep/Rep, and (●) AdAFPep/p53 plus AdAFPep/Rep plus 5-FU. Hep3B cells (1 10^7) were inoculated subcutaneously into the backs of nude mice, and either 220 L of PBS or 2.2 10^8 pfu/220 L of viruses on 7 consecutive days was injected into established tumors when they had grown to 10 mm in diameter. Each experimental group contained five mice. After 7 coinjections, the tumor underwent complete disappearance and never recurred for at least 30 days. Tumor diameters were measured with calipers, and tumor volumes were calculated as described in the Materials and Methods section. Abbreviations: 5-FU, 5-fluorouracil; PBS, phosphate-buffered saline.

respect to the mechanisms of the remarkable antitumor effect, the *in vivo* transactivation of adenoviruses by E1A from the coinfected CRAd has a clear and important role. The synergistic enhancement of oncolysis by CRAd in combination with cytotoxic transgenes, such as p53, is well documented and has also been confirmed in the present study (Figs. 3 and 6).

Even more critical for the antitumor effect found here was 5-FU–mediated augmentation of p53 expression and viral replication. An augmentation of p53 expression through its stabilization by antitumor drugs has been reported previously. Again, the present study clearly confirmed this effect (Fig. 6). In addition, 5-FU facilitated adenovirus replication, leading to an increase in viral release into the culture medium from Hep3B cells infected with AdAFPep/Rep and 5-FU (Fig. 5). It is particularly worth emphasizing that these effects of 5-FU on p53 expression and viral replication were particularly present in the present modality identified in Hep3B cells coinfected with CRAd and RDAdp53 and that they already displayed an increased level of p53 expression and viral replication as a result of the transactivation activity of CRAd. In an *in vivo* setting, the enhancement of p53 function may be beneficial as the protein is known to have antiangiogenetic activity. In fact, CD34 endothelial cells remarkably decreased (Fig. 10A) and the expression of BAI-1, which is a direct target gene of p53, was apparently enhanced (Fig. 10B) in xenografted Hep3B tumors after

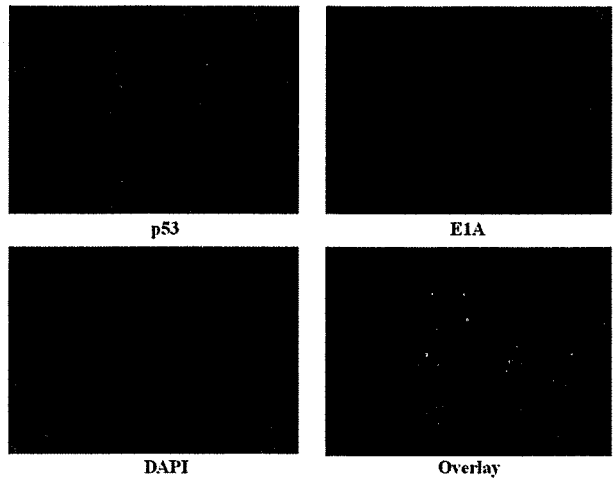

Fig. 9. Coinfection of AdAFPep/p53 and AdAFPep/Rep. Infection of AdAFPep/p53 was assessed with anti-p53 antibody (fluorescein isothiocyanate), and infection of AdAFPep/Rep was detected by anti-E1A antibody (rhodamine). The nucleus was counterstained by DAPI. Coinfection is proven in the overlay panel and indicated by yellow dots. Abbreviations: DAPI, 4 ,6-diamidino-2-phenylindole; E1A, early region 1A.

the treatment of AdAFPep/Rep, AdAFPep/p53, and 5-FU in comparison with those in other treatment groups. This may be an additional and crucial mechanism for antitumor growth. Here we found that the difference between the growth curves of tumors injected *in vivo* with AdAFPep/Rep and AdAFPep/p53 (Fig. 8B) was apparently more distinct than that between the cell survival curves *in vitro* (Fig. 7).

It should be noted that although we successfully suppressed tumor growth for an appreciable period (30 days), the tumor eventually regrew (Fig. 8). This biphasic growth curve may reflect permissive expansion and disappearance of viruses in the tumor nodule because the viral genome was detectable during the growth-suppressed phase (at day 20) but became undetectable after regrowth of the tumor (at day 55; data not shown). The reason for the apparent disappearance of viruses after a certain period of time, though merely speculative, may be immunological elimination as adenoviruses are highly immunogenic.

In addition to viral elimination, immunological reaction to viral components may be a major obstacle in terms of adverse effects when clinical applications of the present strategy are considered. This potential obstacle might be overcome by modification of the fiber and/or hexon or by the use of an adenovirus with a serotype different from those recognized by preexisting antibodies in circulation.[42,43] Alternatively, induction of tolerance to an adenovirus is an attractive strategy that should allow for repeated administration.[44] More recently, it has been reported that it may be possible for the adenovirus vector to target specific cell types selectively, safely, and with little immune response.[45,46]

In conclusion, to the best of our knowledge, this is the first demonstration of the successful management of an

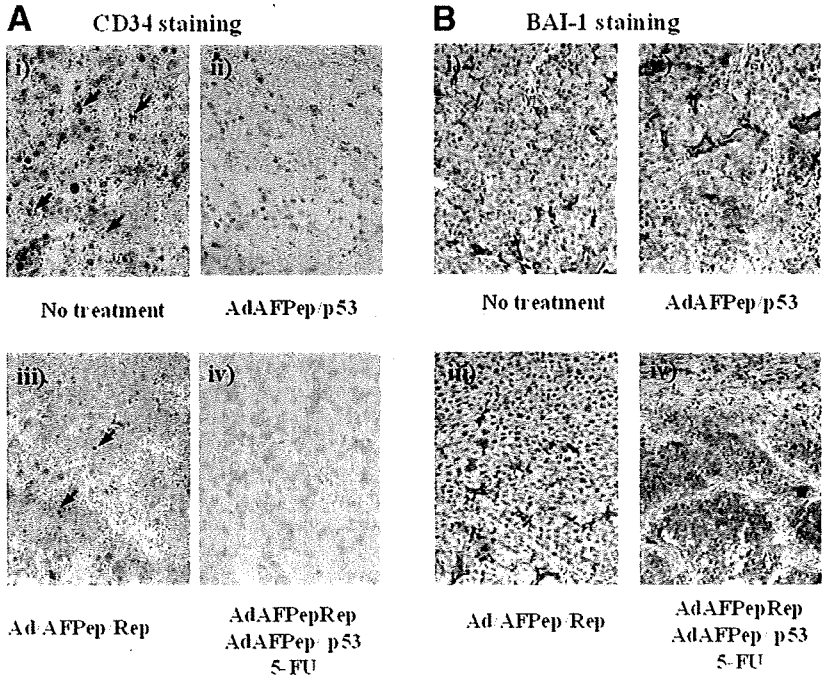

Fig. 10. The immunohistochemical analysis of CD34 and BAI-1. Immunohistochemical staining of tumors was performed with (A) anti-CD34 monoclonal antibody or (B) anti-BAI-1 antibody: (i) no treatment, (ii) AdAFPep/p53, (iii) AdAFPep/Rep, and (iv) AdAFPep/Rep plus AdAFPep/p53 plus 5-FU. (A) Original magnification 400. Arrows indicate CD34 endothelial cells. (B) Original magnification 200. Abbreviations: 5-FU, 5-fluorouracil; BAI-1, brain-specific angiogenesis inhibitor 1.

AFP-producing HCC with a size of 500 mm^3. We believe that the approach that we have developed may hold promise for future clinical applications.

Acknowledgment: We thank Kevin Litton (Bachelor of English Literature) for his assistance with the preparation of this article.

References

1. Llovet J, Ricci S, Mazzaferro V, Hilgard P, Raoul J, Zeuzem S, et al., for the SHARP Investigators Study Group. Sorafenib improves survival in advanced hepatocellular carcinoma (HCC): results of a phase III randomized placebo-controlled trial (SHARP trial) [Abstract]. J Clin Oncol 2007; 25(Suppl):LBA1.
2. Strauss M. Liver-directed gene therapy: prospects and problems. Gene Ther 1994;1:156-164.
3. Schmitz V, Qian C, Ruiz J, Sangro B, Melero I, Mazzolini G, et al. Gene therapy for liver diseases: recent strategies for treatment of viral hepatitis and liver malignancies. Gut 2002;50:130-135.
4. Kanai F, Shiratori Y, Yoshida Y, Wakimoto H, Hamada H, Kanegae Y, et al. Gene therapy for alpha-fetoprotein-producing human hepatoma cells by adenovirus-mediated transfer of the herpes simplex virus thymidine kinase gene. HEPATOLOGY 1996;23:1359-1368.
5. Krohne TU, Shankara S, Geissler M, Roberts BL, Wands JR, Blum HE, et al. Mechanisms of cell death induced by suicide genes encoding purine nucleoside phosphorylase and thymidine kinase in human hepatocellular carcinoma cells in vitro. HEPATOLOGY 2001;34:511-508.
6. Anklesaria P. Gene therapy: a molecular approach to cancer treatment. Curr Opin Mol Ther 2000;2:426-432.
7. Gómez-Navarro J, Curiel DT. Conditionally replicative adenoviral vectors for cancer gene therapy. Lancet Oncol 2000;1:148-158.
8. Habib NA, Sarraf CE, Mitry RR, Havlik R, Nicholls J, Kelly M, et al. E1B-deleted adenovirus (dl1520) gene therapy for patients with primary and secondary liver tumors. Hum Gene Ther 2001;12:219-226.
9. Takahashi M, Sato T, Sagawa T, Lu Y, Sato Y, Iyama S, et al. E1B–55K-deleted adenovirus expressing E1A–13S by AFP-enhancer/promoter is capable of highly specific replication in AFP-producing hepatocellular carcinoma and eradication of established tumor. Mol Ther 2002;5:627-634.
10. Goodrum FD, Ornelles DA. p53 status does not determine outcome of E1B 55-kilodalton mutant adenovirus lytic infection. J Virol 1998;72: 9479-9490.
11. Rothmann T, Hengstermann A, Whitaker NJ, Scheffner M, zur Hausen H. Replication of ONYX-015, a potential anticancer adenovirus, is independent of p53 status in tumor cells. J Virol 1998;72:9470-9478.
12. Turnell AS, Grand RJ, Gallimore PH. The replicative capacities of large E1B-null group A and group C adenoviruses are independent of host cell p53 status. J Virol 1999;73:2074-2083.
13. Harada JN, Berk AJ. p53-Independent and -dependent requirements for E1B–55K in adenovirus type 5 replication. J Virol 1999;73:5333-5344.
14. Ren XW, Liang M, Meng X, Ye X, Ma H, Zhao Y, et al. A tumor-specific conditionally replicative adenovirus vector expressing TRAIL for gene therapy of hepatocellular carcinoma. Cancer Gene Ther 2006;13:159-168.
15. Rodriguez R, Schuur ER, Lim HY, Henderson GA, Simons JW, Henderson DR. Prostate attenuated replication competent adenovirus (ARCA) CN706: a selective cytotoxic for prostate-specific antigen-positive prostate cancer cells. Cancer Res 1997;57:2559-2563.
16. Huang Q, Zhang X, Wang H, Yan B, Kirkpatrick J, Dewhrist MW, et al. A novel conditionally replicative adenovirus vector targeting telomerase-positive tumor cells. Clin Cancer Res 2004;15:1439-1445.
17. Kamizono J, Nagano S, Murofushi Y, Komiya S, Fujiwara H, Matsuishi T, et al. Survivin-responsive conditionally replicating adenovirus exhibits cancer-specific and efficient viral replication. Cancer Res 2005;65:5284-5291.
18. van Beusechem VW, van den Doel PB, Grill J, Pinedo HM, Gerritsen WR. Conditionally replicative adenovirus expressing p53 exhibits enhanced oncolytic potency. Cancer Res 2002;62:6165-6171.
19. Heideman DA, Steenbergen RD, van der Torre J, Scheffner M, Alemany R, Gerritsen WR, et al. Oncolytic adenovirus expressing a p53 variant resistant to degradation by HPV E6 protein exhibits potent and selective replication in cervical cancer. Mol Ther 2005;12:1083-1090.
20. van Beusechem VW, van den Doel PB, Gerritsen WR. Conditionally replicative adenovirus expressing degradation-resistant p53 for enhanced oncolysis of human cancer cells overexpressing murine double minute 2. Mol Cancer Ther 2005;4:1013-1018.
21. Geoerger B, van Beusechem VW, Opolon P, Morizet J, Laudani L, Lecluse Y, et al. Expression of p53, or targeting towards EGFR, enhances the oncolytic potency of conditionally replicative adenovirus against neuroblastoma. J Gene Med 2005;7:584-594.
22. Goldsmith KT, Dion LD, Curiel DT, Garver RI Jr. Trans E1 component requirements for maximal replication of E1-defective recombinant adenovirus. Virology 1998;248:406-419.
23. Lee CT, Park KH, Yanagisawa K, Adachi Y, Ohm JE, Nadaf S, et al. Combination therapy with conditionally replicating adenovirus and replication defective adenovirus. Cancer Res 2004;64:6660-6665.
24. Nakano K, Todo T, Zhao G, Yamaguchi K, Kuroki S, Cohen JB, et al. Enhanced efficacy of conditionally replicating herpes simplex virus (G207) combined with 5-fluorouracil and surgical resection in peritoneal cancer dissemination models. J Gene Med 2005;7:638-648.
25. Eisenberg DP, Adusumilli PS, Hendershott KJ, Yu Z, Mullerad M, Chan MK, et al. 5-Fluorouracil and gemcitabine potentiate the efficacy of oncolytic herpes viral gene therapy in the treatment of pancreatic cancer. J Gastrointest Surg 2005;9:1068-1077.
26. Bernt KM, Steinwaerder DS, Ni S, Li ZY, Roffler SR, Lieber A. Enzyme-activated prodrug therapy enhances tumor-specific replication of adenovirus vectors. Cancer Res 2002;62:6089-6098.
27. Damia G, Filiberti L, Vikhanskaya F, Carrassa L, Taya Y, D'Incalci M, et al. Cisplatinum and taxol induce different patterns of p53 phosphorylation. Neoplasia 2001;3:10-16.
28. Doronin K, Kuppuswamy M, Toth K, Tollefson AE, Krajcsi P, Krougliak V, et al. Tissue-specific, tumor-selective, replication-competent adenovirus vector for cancer gene therapy. J Virol 2001;75:3314-3324.
29. Modesitt SC, Ramirez P, Zu Z, Bodurka-Bevers D, Gershenson D, Wolf JK. In vitro and in vivo adenovirus-mediated p53 and p16 tumor suppressor therapy in ovarian cancer. Clin Cancer Res 2001;7:1765-1772.
30. Vollmer CM, Ribas A, Butterfield LH, Dissette VB, Andrews KJ, Eilber FC, et al. p53 selective and nonselective replication of an E1B-deleted adenovirus in hepatocellular carcinoma. Cancer Res 1999;59:4369-4374.
31. Ohashi M, Kanai F, Tateishi K, Taniguchi H, Marignani PA, Yoshida Y, et al. Target gene therapy for alpha-fetoprotein-producing hepatocellular carcinoma by E1B55k-attenuated adenovirus. Biochem Biophys Res Commun 2001;282:529-535.
32. Fukunaga K, Arita M, Takahashi M, Morris AJ, Pfeffer M, Levy BD. Identification and functional characterization of a presqualene diphosphate phosphatase. J Biol Chem 2006;281:9490-9497.
33. Scaglioni P, Melegari M, Takahashi M, Chowdhury JR, Wands J. Use of dominant negative mutants of the hepadnaviral core protein as antiviral agents. HEPATOLOGY 1996;24:1010-1017.
34. Yamano S, Tokino T, Yasuda M, Kaneuchi M, Takahashi M, Niitsu Y, et al. Induction of transformation and p53-dependent apoptosis by adenovirus type 5 E4orf6/7 cDNA. J Virol 1999;73:10095-10103.
35. Igarashi T, Suzuki S, Takahashi M, Tamaoki T, Shimada T. A novel strategy of cell targeting based on tissue-specific expression of the ecotropic retrovirus receptor gene. Hum Gene Ther 1998;9:2691-2698.
36. Mosmann T. Rapid colorimetric assay for cellular growth and survival: application to proliferation and cytotoxicity assays. J Immunol Methods 1983;65:55-63.
37. Ferrari M, Fornasiero MC, Isetta AM. MTT colorimetric assay for testing macrophage cytotoxic activity in vitro. J Immunol Methods 1990;131: 165-172.

38. Yamamoto M, Davydova J, Wang M, Siegal GP, Krasnykh V, Vickers SM, et al. Infectivity enhanced, cyclooxygenase-2 promoter-based conditionally replicative adenovirus for pancreatic cancer. Gastroenterology 2003; 125:1203-1218.
39. Chou TC, Talalay P. Quantitative analysis of dose-effect relationships: the combined effects of multiple drugs or enzyme inhibitors. Adv Enzyme Regul 1984;22:27-55.
40. Kijima T, Osaki T, Nishino K, Kumagai T, Funakoshi T, Goto H, et al. Application of the Cre recombinase/loxP system further enhances antitumor effects in cell type-specific gene therapy against carcinoembryonic antigen-producing cancer. Cancer Res 1999;59:4906-4911.
41. Ahn WS, Han YJ, Bae SM, Kim TH, Rho MS, Lee JM, et al. Differential suppression of human cervical cancer cell growth by adenovirus delivery of p53 in vitro: arrest phase of cell cycle is dependent on cell line. Jpn J Cancer Res 2002;93:1012-1019.
42. Nakamura T, Sato K, Hamada H. Reduction of natural adenovirus tropism to the liver by both ablation of fiber-coxsackievirus and adenovirus receptor interaction and use of replaceable short fiber. J Virol 2003;77: 2512-2521.
43. Dehari H, Ito Y, Nakamura T, Kobune M, Sasaki K, Yonekura N, et al. Enhanced antitumor effect of RGD fiber-modified adenovirus for gene therapy of oral cancer. Cancer Gene Ther 2003;10:75-85.
44. Chen P, Kovesdi I, Bruder JT. Effective repeat administration with adenovirus vectors to the muscle. Gene Ther 2000;7:587-595.
45. Shalev M, Kadmon D, Teh BS, Butler EB, Aguilar-Cordova E, Thompson TC, et al. Suicide gene therapy toxicity after multiple and repeat injections in patients with localized prostate cancer. J Urol 2000;163:1747-1750.
46. Shimada H, Matsubara H, Shiratori T, Shimizu T, Miyazaki S, Okazumi S, et al. Phase I/II adenoviral p53 gene therapy for chemoradiation resistant advanced esophageal squamous cell carcinoma. Cancer Sci 2006;97:554-561.

Association of visceral fat accumulation and plasma adiponectin with rectal dysplastic aberrant crypt foci in a clinical population

Hirokazu Takahashi,[1,5] Tetsuji Takayama,[2] KyokoYoneda,[1] Hiroki Endo,[1] Hiroshi Iida,[1] Michiko Sugiyama,[1] Koji Fujita,[1] Masato Yoneda,[1] Masahiko Inamori,[1] Yasunobu Abe,[1] Satoru Saito,[1] Koichiro Wada,[3] Hitoshi Nakagama[4] and Atsushi Nakajima[1]

[1]Gastroenterology Division, Yokohama City University Graduate School of Medicine, Yokohama, Kanagawa 236-0004; [2]Gastroenterology Division, University of Tokushima Faculty of Medicine, Tokushima 770-8503; [3]Department of Pharmacology, School of Dentistry, Osaka University, Osaka 565-0871; [4]Biochemistry Division, National Cancer Center Research Institute, Tokyo 104-0045, Japan

(Received June 21, 2008/Revised August 31, 2008/Accepted September 5, 2008/Online publication October 23, 2008)

The association between obesity and the risk of colorectal cancer (CRC) cannot be easily evaluated because CRC itself is associated with a gradual loss of bodyweight. Aberrant crypt foci (ACF) can be classified as dysplastic ACF or non-dysplastic ACF by magnifying colonoscopy, and dysplastic ACF are thought to be a biomarker of CRC. Ninety-four participants who underwent colonoscopy at Yokohama City University Hospital, Japan, were enrolled in the current study. We detected 557 ACF, including 67 dysplastic ACF (12.0%). Univariate regression analysis was conducted to determine correlations between the number of dysplastic ACF and various potential risk factors, including patient age, waist circumference, body mass index, visceral fat area (VFA), and plasma adiponectin level. The results of multiple regression analysis revealed that the number of dysplastic ACF correlated with age (correlation coefficient $r = 0.212$, $P = 0.0383$) and plasma adiponectin level ($r = -0.201$, $P = 0.0371$), even after adjustments for sex, waist circumference, body mass index, and VFA. Our univariate correlation analysis data showed a significant correlation with the number of dysplastic ACF with VFA ($r = 0.238$, $P = 0.0209$), no correlation with subcutaneous fat area, and an inverse correlation with the plasma level of adiponectin ($r = -0.258$, $P = 0.0118$). Thus, our results suggest that aging and visceral fat accumulation could correlate moderately with colorectal carcinogenesis. The novelty of our study lies in the finding that visceral fat accumulation and a low plasma adiponectin level may promote colorectal carcinogenesis; therefore, these obesity-related parameters may serve as novel targets for CRC prevention. (*Cancer Sci* 2009; 100: 29–32)

Obesity and its associated visceral fat accumulation have been reported to be linked to an elevated risk of cardiovascular disease, diabetes mellitus, and mortality, and these complications are rapidly becoming significant problems.[1,2] Visceral adipose tissue is not only fat storage tissue, but also a metabolically active organ secreting many adipocytokines, such as adiponectin.[3] Obesity is reportedly an important risk factor for CRC.[4] CRC has high mortality and morbidity rates, and its prevalence has been increasing.[5,6] The precise risk factors for CRC remain unclear, although a family history and several dietary and lifestyle factors have been proposed to be involved.[7]

The association between obesity and the risk of CRC cannot be easily evaluated because of the confounding effect of bodyweight loss with CRC. Therefore, we sought to identify a biomarker for risk assessment and monitoring of CRC. ACF, which were first discovered in mice treated with azoxymethane,[8] have been clearly shown to be precursor lesions of CRC, and are now established as a biomarker of the risk of CRC in azoxymethane-treated mice and rats.[9] In humans, ACF can be classified as dysplastic or non-dysplastic through the use of magnifying colonoscopy.[10] ACF have not been firmly established to be precursors of CRC; however, dysplastic ACF could possibly serve as a biomarker of the risk of CRC. Previous studies have reported that individuals with CRC have more ACF than those without CRC, therefore dysplastic ACF represent potential clinical precursors of CRC and colorectal adenoma.[11–14] Recently, an association was suggested to exist between obesity and the risk of CRC.[15,16] However, the relationship between obesity and ACF remains unclear. Therefore, the current study in a clinical population aimed to investigate the relationship between various obesity-associated parameters and rectal dysplastic ACF.

Patients and Methods

Study population. We prospectively evaluated 94 subjects recruited from the population of healthy individuals who underwent colonoscopy at Yokohama City University Hospital, Japan. The exclusion criteria included: presence of contraindications to colonoscopy; current or past non-steroidal anti-inflammatory drug use including aspirin; family history of CRC; or history of adenoma, carcinoma, familial adenomatous polyposis, inflammatory bowel disease, or radiation colitis. Subjects with a history of colectomy, gastrectomy, or colorectal polypectomy, and those treated with daily insulin self-injection or sulfonylurea for diabetes mellitus, were also excluded. In order to investigate the influence of obesity on colorectal carcinogenesis, patients with colorectal adenoma or carcinoma at the time of colonoscopy were also excluded from the study. Written informed consent was obtained from all subjects prior to their participation. The study protocol was approved by the Yokohama City University Hospital Ethics Committee.

Collection and analysis of blood samples for adiponectin level. Blood samples were obtained in the morning on the day of colonoscopy after overnight fasting. Plasma adiponectin levels were measured by enzyme-linked immunosorbent assay of the total forms of human adiponectin (SRL Co., Tokyo, Japan).

Magnifying colonoscopy for identification of ACF. Participants' bowel preparation for the colonoscopy was carried out using

[5]To whom correspondence should be addressed.
E-mail: hirokazu@med.yokohama-cu.ac.jp
Abbreviations: ACF, aberrant crypt foci; BMI, body mass index; CRC, colorectal cancer; CT, computed tomography; SFA, subcutaneous fat area; TFA, total fat area; VFA, visceral fat area.

doi: 10.1111/j.1349-7006.2008.00994.x

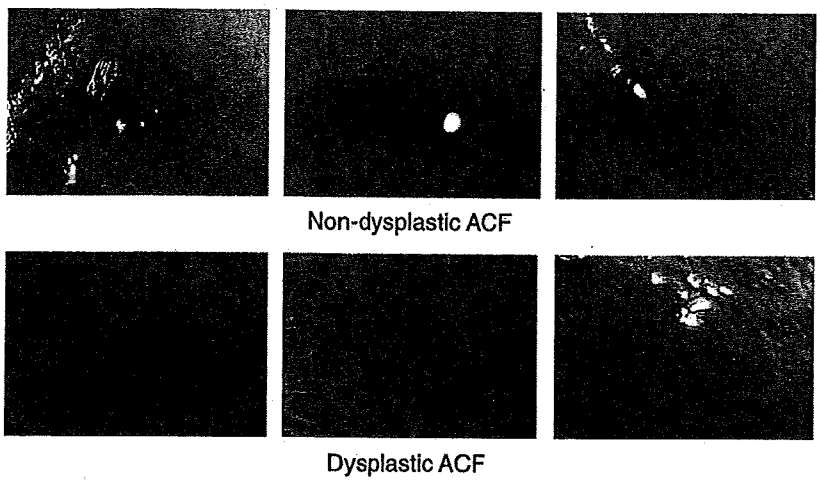

Fig. 1. Typical features of non-dysplastic and dysplastic aberrant crypt foci (ACF) on magnifying colonoscopy after methylene blue staining.

polyethylene glycol solution. A Fujinon EC-490ZW5/M colonoscope was used for the magnifying colonoscopy (Fujinon Toshiba ES Systems, Tokyo, Japan). Total colonoscopy was carried out before imaging of rectal ACF. Subsequently, 0.25% methylene blue was applied to the mucosa with a spray catheter. Aberrant crypts were distinguished from normal crypts by their deeper staining and larger diameter, and the number of ACF in the rectum was counted. This counting was conducted in the lower rectal region, extending from the middle Houston valve to the dentate line, based on the results of a previous study.[10] All ACF were recorded photographically and evaluated by two independent observers who were unaware of the subjects' clinical histories.

Criteria used for endoscopic diagnosis. ACF were defined as lesions in which the crypts were more darkly stained with methylene blue than normal crypts and had larger diameters, often with oval or slit-like lumens and a thicker epithelial lining.[17–20] Dysplastic ACF were defined as crypts in which each lumen was compressed or not distinct, with an epithelial lining that was much thicker than that of normal surrounding crypts. Non-dysplastic ACF were classified as hyperplastic or non-hyperplastic.[10]

Measurement of VFA and SFA. BMI was calculated using the following equation: bodyweight (kg)/(height [m]^2). Intra-abdominal adipose tissue was assessed, as described previously by measuring the VFA, SFA, TFA, and waist circumference from CT images at the level of the umbilicus.[4,10] All CT scans were carried out with the subjects in the supine position. The borders of the intra-abdominal cavity were outlined on the CT images, and the VFA was quantified using Fat Scan software (N2 System Corporation, Kobe, Japan).

Statistical analysis. We examined the associations between the risk factors for CRC and the number of dysplastic ACF. All data were expressed as mean ± SD, unless otherwise indicated. The relationships between the number of dysplastic ACF and relevant covariates were examined by univariate regression analysis, and standardized correlation coefficients were determined using Stat View software (SAS Institute, Cary, NC, USA). Multiple regression analysis was carried out to assess the relationship between the number of dysplastic ACF and potentially associated variables, and to determine the standardized correlation coefficients. The dependent variable was the number of dysplastic ACF, and the independent variables were age, sex, VFA, and plasma adiponectin level. Waist circumference and BMI were excluded from this analysis because these factors have a high correlation with VFA. P-values < 0.05 were considered to denote statistical significance.

Results

Colonoscopic features of ACF. A total of 557 ACF, including 67 dysplastic ACF, were counted by magnifying colonoscopy in the 94 patients. The aberrant crypts were larger, thicker, and more darkly stained than the normal crypts. Dysplastic ACF and non-dysplastic ACF accounted for 12.0% (67 of 557) and 88.0% (490 of 557) of the total, respectively. The number of subjects with dysplastic ACF was 34, and the number with non-dysplastic ACF was 76. In the lesions detected by magnifying colonoscopy, the size (i.e. median number of crypts ± SD) per ACF was 15.1 ± 10.4 and per dysplastic ACF was 8.5 ± 11.8. The average number of composition crypts per ACF was 93.2 ± 124.3 and per dysplastic ACF was 16.3 ± 26.2. In the 94 patients, the mean total number of ACF (non-dysplastic and dysplastic) per patient was 5.92 ± 6.50, and the mean number of dysplastic ACF per patient was 0.71 ± 1.16. The typical colonoscopic features of dysplastic and non-dysplastic ACF are shown in Figure 1.

Patient characteristics. The clinical characteristics of the study participants are shown in Table 1. The mean age was 65.1 ± 10.8 years, and there were 48 men and 46 women. The mean waist circumference, BMI, TFA, VFA, SFA, and plasma adiponectin level were 86.3 ± 10.0 cm, 23.3 ± 3.1 kg/m^2, 200.8 ± 91.4 cm^2, 83.9 ± 50.1 cm^2, 116.7 ± 60.4 cm^2, and 11.0 ± 5.6 μg/mL, respectively.

Univariate regression analysis: Correlations between risk factors for CRC and the number of dysplastic ACF. Age correlated significantly with the number of dysplastic ACF, as shown in Table 2 ($r = 0.232$, $P = 0.0242$). Sex showed no correlation with the number of dysplastic ACF. All of the obesity parameters, except SFA ($r = -0.001$, $P = 0.9979$), correlated significantly with the number of dysplastic ACF, as follows: waist circumference ($r = 0.225$, $P = 0.0293$), BMI ($r = 0.307$, $P = 0.0325$), and VFA ($r = 0.238$, $P = 0.0209$). The plasma level of adiponectin showed a significant inverse correlation with the number of dysplastic ACF ($r = -0.258$, $P = 0.0118$). Age was the only parameter that correlated significantly with the number of non-dysplastic ACF ($r = 0.218$, $P = 0.0336$), which were much more abundant than dysplastic ACF in the study subjects.

Multiple regression analysis: Correlations between risk factors for CRC and the number of dysplastic ACF. The results of the multiple regression analysis are shown in Table 3. After adjustments for sex, waist circumference, BMI, and VFA, the parameters of age and plasma adiponectin level still correlated significantly with the number of dysplastic ACF ($P = 0.0383$ and $P = 0.0371$, respectively).

doi: 10.1111/j.1349-7006.2008.00994.x

Table 1. Clinical characteristics of study participants

Characteristic	Overall	Subjects with non-dysplastic ACF	Subjects with dysplastic ACF
Number	94	76	34
Age (years)	65.1 ± 10.8	66.3 ± 10.1	66.2 ± 8.1
Sex (male : female)	48:46	43:33	21:13
Waist circumference (cm)	86.3 ± 10.0	86.0 ± 10.5	88.4 ± 11.2
Body mass index (kg/m²)	23.3 ± 3.1	23.3 ± 3.2	24.2 ± 3.0
Total fat area (cm²)	200.8 ± 91.4	199.5 ± 95.7	222.0 ± 96.0
Visceral fat area (cm²)	83.9 ± 50.1	86.3 ± 51.6	103.6 ± 52.6
Ssubcutaneous fat area (cm²)	116.7 ± 60.4	112.9 ± 60.8	117.8 ± 58.4
Plasma adiponectin (μg/mL)	11.0 ± 5.6	11.3 ± 5.8	9.4 ± 4.3

Data are expressed as mean ± SD. ACF, aberrant crypt foci.

Table 2. Univariate correlation analysis: Correlations between the number of non-dysplastic or dysplastic aberrant crypt foci (ACF) and the risk factors for colorectal cancer

Risk factor	Non-dysplastic ACF		Dysplastic ACF	
	r	*P*	*r*	*P*
Age	0.218	0.0336*	0.232	0.0242*
Sex	0.109	0.2928	0.087	0.4069
Waist circumference	0.076	0.4651	0.225	0.0293*
Body mass index	0.169	0.1011	0.307	0.0325*
Total fat area	0.126	0.2257	0.135	0.1941
Visceral fat area	0.137	0.1868	0.238	0.0209*
Subcutaneous fat area	0.078	0.4560	−0.001	0.9979
Plasma adiponectin	−0.019	0.8538	−0.258	0.0118*

Age, waist circumference, body mass index, visceral fat area, and plasma adiponectin level correlated with the number of dysplastic ACF.
*$P < 0.05$.

Table 3. Multiple regression analysis: Correlations between the number of dysplastic aberrant crypt foci and the risk factors for colorectal cancer

Risk factor	Correlation coefficient	*P*
Age	0.212	0.0383*
Sex	0.038	0.7141
Waist circumference	−0.152	0.4508
Body mass index	0.249	0.1618
Visceral fat area	0.089	0.5807
Plasma adiponectin	−0.201	0.0371*

R^2 for the entire model = 0.368.
After adjustments for sex, waist circumference, body mass index, and visceral fat area, the parameters of age and plasma adiponectin level still correlated with the number of dysplastic aberrant crypt foci.
*$P < 0.05$.

Discussion

In the present study a total of 557 ACF were counted in the 94 patients, and we demonstrated a significant correlation between the number of dysplastic ACF and the VFA, and a significant inverse correlation between the number of dysplastic ACF and the plasma adiponectin level. Age was also associated with the number of ACF, that is, the number of dysplastic and non-dysplastic ACF increased with age. CRC is thought to progress through several morphological stages, from the formation of polyps to the onset of malignant change.[21] Genetic alterations, including mutations in the *K-ras*, *p53*, and *APC* genes, have been reported to be associated with the disease progression.[22] The *K-ras* mutation has also been reported in human ACF.[23] Therefore, the increased risk of ACF formation with age may be influenced mainly by these genetic alterations. Sex showed no correlation with the number of dysplastic ACF in the present study; however, the incidence of CRC is lower in women than in men.[24,25] It has been suggested that the initiation of dysplastic ACF is comparable in men and women, but thereafter tumor progression differs because visceral fat accumulation is higher in men than woman. This visceral fat accumulation may affect tumor progression.

Waist circumference has often been suggested to be associated with VFA. Consistent with this suggestion, our data showed that both waist circumference and VFA were associated with the number of dysplastic ACF. Recent reports have suggested that obesity may be associated with a high risk of CRC.[4] Several studies have shown that increased BMI is associated with an increased risk of CRC.[26] The importance of the size of ACF has been reported,[27] and the correlation between size, measured as the median number of crypts per both non-dysplastic ACF and dysplastic ACF, and risk factors was analyzed. The correlation between the median number of crypts per ACF and any risk factors had almost the same result as the number of ACF (data not shown). Our data showed a direct correlation between the VFA and the number of dysplastic ACF, and an inverse correlation between the plasma adiponectin level and the number of dysplastic ACF (Table 2). A previous study showed that the *K-ras* gene was mutated in 50–60% of patients with dysplastic ACF,[10] thus genetic alterations were already underway. Visceral fat correlated with dysplastic ACF in the current study, and another study showed that increased visceral adiposity was a significant predictor of lower rates of disease-free survival in patients with resectable colorectal cancer,[28] suggesting that visceral fat plays an important role in colorectal carcinogenesis and progression. Visceral fat tissue is known to be an endocrine organ that secretes adiponectin, which has an inverse relationship with obesity and visceral fat.[29] We carried out multiple regression analysis to assess whether plasma adiponectin may be a risk factor for dysplastic ACF growth, independent of the effects of obesity. If dysplastic ACF are a biomarker of the risk of colorectal adenoma and CRC, then some factors associated with the risk of CRC may also influence the number of dysplastic ACF. Very little is known about the factors that initiate or promote the growth of dysplastic ACF in humans. Our results suggest that plasma adiponectin levels are inversely associated with the number of ACF, and that visceral fat may be associated directly with ACF and thus could be a risk factor for the early stage of colorectal carcinogenesis.

There are many reports on the existence of relationships between the risk of CRC and exercise, energy use, glycemic index, and food choices and dietary constituents.[30–32] These factors affect each other, therefore it is difficult to evaluate the relationship between any one factor and the risk of CRC. Obesity

is thought to result from many of these factors. It is also thought that aging, visceral fat, and adiponectin are important in CRC carcinogenesis. Further investigation is needed to elucidate the mechanisms that affect these relationships and the impact on the development of CRC.

The novelty of our study lies in our use of dysplastic ACF as a biomarker for risk of CRC to show that visceral fat accumulation and low plasma adiponectin level may affect colorectal carcinogenesis. Further studies should be conducted to clarify the role that visceral fat accumulation and reduced plasma adiponectin play in dysplastic ACF growth and whether these obesity-related parameters may serve as novel targets for CRC prevention.

Acknowledgments

We thank Machiko Hiraga for her technical assistance. This work was supported in part by a Grant-in-Aid for research on the Third Term Comprehensive Control Research for Cancer from the Ministry of Health, Labour, and Welfare, Japan to A.N., a grant from the National Institute of Biomedical Innovation to A.N., a grant from the Ministry of Education, Culture, Sports, Science, and Technology, Japan (KIBAN-B) to A.N., a grant from the Ministry of Education, Culture, Sports, Science, and Technology, Japan (WAKATE-B) to H.T., a research grant from the Princess Takamatsu Cancer Research Fund to A.N., and a grant for the 2007 Strategic Research Project (no. K19041) of Yokohama City University, Japan to H.T. and A.N.

References

1 Fujioka S, Matsuzawa Y, Tokunaga K *et al.* Contribution of intra-abdominal fat accumulation to the impairment of glucose and lipid metabolism in human obesity. *Metabolism* 1987; **36**: 54–9.
2 Kissebah AH, Vydelingum N, Murray R *et al.* Relation of body fat distribution to metabolic complications of obesity. *J Clin Endocrinol Metab* 1982; **54**: 254–60.
3 Park KG, Park KS, Kim MJ *et al.* Relationship between serum adiponectin and leptin concentrations and body fat distribution. *Diabetes Res Clin Pract* 2004; **63**: 135–42.
4 Giovannucci E, Aasherio A, Rimm EB *et al.* Physical activity, obesity, and risk for colon cancer and adenoma in men. *Ann Intern Med* 1995; **122**: 327–34.
5 Anderson WF, Umar A, Brawley OW. Colorectal carcinoma in black and white race. *Cancer Metastasis Rev* 2003; **22**: 67–82.
6 Rougier P, Mitry E. Epidemiology, treatment and chemoprevention in colorectal cancer. *Ann Oncol* 2003: **14**: ii3–5.
7 Garland C, Shekelle RB, Barrett-Connor E *et al.* Dietary vitamin D and calcium and risk of colorectal cancer: a 19-year prospective study in men. *Lancet* 1985; **1**: 307–9.
8 Bird RP. Observation and quantification of aberrant crypts in the murine colon treated with a colon carcinogen: preliminary findings. *Cancer Lett* 1987; **37**: 147–51.
9 Pretlow TP, O'Riordan MA, Somich GA *et al.* Aberrant crypts correlate with tumor incidence in F344 rats treated with azoxymethane and phytate. *Carcinogenesis* 1992; **13**: 1509–12.
10 Takayama T, Katsuki S, Takahashi Y *et al.* Aberrant crypt foci of the colon as precursors of adenoma and cancer. *N Engl J Med* 1998; **339**: 1277–84.
11 Nascimbeni R, Villanacci V, Mariani PP *et al.* Aberrant crypt foci in the human colon: frequency and histologic patterns in patients with colorectal cancer or diverticular disease. *Am J Surg Pathol* 1999; **23**: 1256–63.
12 Shpitz B, Bomstein Y, Mekori Y *et al.* Aberrant crypt foci in human colons: distribution and histomorphologic characteristics. *Hum Pathol* 1998; **29**: 469–75.
13 Adler DG, Gostout CJ, Sorbi D *et al.* Endoscopic identification and quantification of aberrant crypt foci in the human colon. *Gastrointest Endosc* 2002; **56**: 657–62.
14 Nucci MR, Robinson CR, Longo P *et al.* Phenotypic and genotypic characteristics of aberrant crypt foci in human colorectal mucosa. *Hum Pathol* 1997; **28**: 1396–407.
15 Gunter MJ, Leitzmann MF. Obesity and colorectal cancer: epidemiology, mechanisms and candidate genes. *J Nutr Biochem* 2006; **17**: 145–56.
16 Otake S, Takeda H, Suzuki Y *et al.* Association of visceral fat accumulation and plasma adiponectin with colorectal adenoma: evidence for participation of insulin resistance. *Clin Cancer Res* 2005; **11**: 3642–6.
17 Roncucci L, Stamp D, Medline A *et al.* Identification and quantification of aberrant crypt foci and microadenomas in the human colon. *Hum Pathol* 1991; **22**: 287–94.
18 Roncucci L, Medline A, Bruce WR. Classification of aberrant crypt foci and microadenomas in human colon. *Cancer Epidemiol Biomarkers Prev* 1991; **1**: 57–60.
19 Pretlow TP, Barrow BJ, Ashton WS *et al.* Aberrant crypts: putative preneoplastic foci in human colonic mucosa. *Cancer Res* 1991; **51**: 1564–7.
20 Pretlow TP, O'Riordan MA, Pretlow TG *et al.* Aberrant crypts in human colonic mucosa: putative preneoplastic lesions. *J Cell Biochem Suppl* 1992; **16**: 55–62.
21 Kinzler KW, Vogelstein B. Lessons from hereditary colorectal cancer. *Cell* 1996; **87**: 159–70.
22 Fearon ER, Vogelstein B. A genetic model for colorectal tumorigenesis. *Cell* 1990; **61**: 759–67.
23 Yuan P, Sun MH, Zhang JS *et al.* APC and K-ras gene mutation in aberrant crypt foci of human colon. *World J Gastroenterol* 2001; **7**: 352–6.
24 Gao RN, Neutel CI, Wai E. Gender differences in colorectal cancer incidence, mortality, hospitalizations and surgical procedures in Canada. *J Public Health* 2008; **30**: 194–201.
25 de Kok IM, Wong CS, Chia KS *et al.* Gender differences in the trend of colorectal cancer incidence in Singapore, 1968–2002. *Int J Colorectal Dis* 2008; **23**: 461–7.
26 Graham S, Marshall J, Haughey B *et al.* Dietary epidemiology of cancer of the colon in western New York. *Am J Epidemiol* 1988; **128**: 490–503.
27 Rudolph RE, Dominitz JA, Lampe JW *et al.* Risk factors for colorectal cancer in relation to number and size of aberrant crypt foci in humans. *Cancer Epidemiol Biomarkers Prev* 2005; **14**: 605–8.
28 Moon HG, Ju YT, Jeong CY *et al.* Visceral obesity may affect oncologic outcome in patients with colorectal cancer. *Ann Surg Oncol* 2008; **15**: 1918–22.
29 Arita Y, Kihara S, Ouchi N *et al.* Paradoxical decrease of an adipose-specific protein, adiponectin, in obesity. *Biochem Biophys Res Commun* 1999; **257**: 79–83.
30 Gerhardsson M, Floderus B, Norell SE. Physical activity and colon cancer risk. *Int J Epidemiol* 1988; **17**: 743–6.
31 Slattery ML, Benson J, Berry TD *et al.* Dietary sugar and colon cancer. *Cancer Epidemiol Biomarkers Prev* 1997; **6**: 677–85.
32 Reedy J, Haines PS, Steckler A *et al.* Qualitative comparison of dietary choices and dietary supplement use among older adults with and without a history of colorectal cancer. *J Nutr Educ Behav* 2005; **37**: 252–8.

doi: 10.1111/j.1349-7006.2008.00994.x

J Gastroenterol (2009) 44:964–975
DOI 10.1007/s00535-009-0089-8

ORIGINAL ARTICLE—LIVER, PANCREAS, AND BILIARY TRACT

Suppressive effect of sulindac on branch duct-intraductal papillary mucinous neoplasms

Tsuyoshi Hayashi · Hirotoshi Ishiwatari · Hideyuki Ihara · Yutaka Kawano · Koichi Takada · Koji Miyanishi · Masayoshi Kobune · Rishu Takimoto · Tomoko Sonoda · Tetsuji Takayama · Junji Kato · Yoshiro Niitsu

Received: 4 February 2009 / Accepted: 29 April 2009 / Published online: 18 June 2009

Abstract
Backgound When considering surgery for branch duct-intraductal papillary mucinous neoplasms (BD-IPMNs) with suspected malignancy, it should be recognized that these lesions are frequently multifocal and are usually found in elderly patients with potential comorbidities that could affect the outcome of surgery. Clinical trials of chemoprevention have been conducted for a wide variety of malignancies.
Methods Twenty-two BD-IPMN patients participated in the trial at our institution from June 2004 to January 2007. Ten of the 22 patients who rejected surgical therapy although their lesions or clinical symptoms met the criteria for surgical resection of the International Association of Pancreatology guidelines were assigned to the treatment group. Sulindac (150 mg twice daily) and omeprazole (20 mg once daily) were administered to these patients for 18 months. The remaining 12 patients comprised the control group. Branch duct diameter and mural nodule heights were monitored by either magnetic resonance cholangiopancreatography (MRCP) or computed tomography (CT) and by endoscopic ultrasonography (EUS).
Results Both branch duct diameter and mural nodule height of BD-IPMNs in the treatment group were significantly reduced, while those in the control group were unchanged. Immunohistochemical staining for cyclooxygenase-1 and -2 was negative in hyperplasia, adenoma and carcinoma portions of resected pancreatic specimens but was clearly positive for glutathione-*S*-transferase π (GST-π), suggesting that GST-π is a putative target molecule for sulindac.
Conclusions Although a larger scale randomized controlled study is needed in future, the present results suggest the promise of chemoprevention of carcinoma derived from BD-IPMNs by sulindac.

Keywords Intraductal papillary-mucinous neoplasm · Chemoprevention · Non-steroidal anti-inflammatory drugs · Glutathione-*S*-transferase π

Abbreviations

IAP	International Association of Pancreatology
BD-IPMNs	Branch duct intraductal papillary-mucinous neoplasm
MD-IPMN	Main duct intraductal papillary-mucinous neoplasm
ERP	Endoscopic retrograde pancreatography
CT	Computed tomography
MRCP	Magnetic resonance cholangiopancreatography
EUS	Endoscopic ultrasonography
NSAIDs	Non-steroidal anti-inflammatory drugs

T. Hayashi · H. Ishiwatari · H. Ihara · Y. Kawano · K. Takada · K. Miyanishi · M. Kobune · R. Takimoto · J. Kato
Fourth Department of Internal Medicine,
Sapporo Medical University School of Medicine,
Sapporo, Japan

T. Sonoda
Department of Public Health, Sapporo Medical University School of Medicine, Sapporo, Japan

T. Takayama
Department of Gastroenterology and Oncology,
Institute of Health Biosciences,
The University of Tokushima Graduate School,
Sapporo, Japan

Y. Niitsu (✉)
Department of Molecular Target Exploration,
Sapporo Medical University School of Medicine,
South-1, West-16 Chuo-ku Sapporo,
Hokkaido 060-8556, Japan
e-mail: niitsu@sapmed.ac.jp

COX-1	Cyclooxygenase-1
COX-2	Cyclooxygenase-2
GST-π	Glutathione-*S*-transferase π

Introduction

Over the past 15 years, mostly due to developments in high-resolution abdominal imaging techniques, the number of patients found to have intraductal papillary mucinous neoplasms (IPMNs) has dramatically increased. IPMNs can be categorized into two groups based on a topographical difference: neoplasms arising from the main pancreatic duct (MD-IPMNs) and IPMNs involving only the secondary branch ducts (BD-IPMNs). Recent studies have revealed that these two types of IPMNs also differ with regard to biological behavior, such as invasiveness and expansion rate [1]. The prevalence of cancer among MD-IPMNs and BD-IPMNs ranges from 57–92% to 6–46%, respectively, indicating immediate surgical resection for the former lesion [2–5]. As to the therapeutic strategy for the latter lesion, the International Association of Pancreatology (IAP) suggests that patients with no symptoms, with a branch duct diameter of <30 mm, with no mural nodules and a main pancreatic duct diameter <6 mm can be followed with periodic imaging and that patients who develop any one of those four findings should undergo surgery [6]. However, when considering surgery for BD-IPMNs, it should be noted that the lesions are frequently multifocal, are usually found in elderly patients with potential comorbidities that can affect the outcome after surgery, and are associated with a high incidence of extra pancreatic malignancies.

Clinical trials of chemoprevention have been conducted for a wide variety of malignancies, including colorectal cancer, lung cancer, etc. [7–10]. Since chemoprevention is a more active approach than the simple watch and wait follow-up for non-operative BD-IPMNs and is considered to be suitable for avoiding the difficulties described above, in the present study, we attempted to treat patients with BD-IPMNs who had refused surgery with a non-steroidal anti-inflammatory drugs (NSAIDs), sulindac, which has been used to suppress the growth of pancreatic cancer cell line and to prevent the occurrence of pancreatic neoplasia [11–13].

Methods

Clinical trial of sulindac administration to patients with IPMNs

This clinical trial was approved by Institutional Review Board of Sapporo Medical University. Written informed consent was obtained from all enrolled subjects.

Forty patients were diagnosed to have BD-IPMNs, which were grape-like multilocular cysts with a communication to the main pancreatic duct, based on results of magnetic resonance cholangiopancreatography (MRCP) or computed tomography (CT) at our institution from June 2004 to January 2007. Of these, a total of 22 patients entered into the trial. Ten of these 22 patients had refused surgical therapy although their lesions or clinical symptoms met the criteria for surgical resection as defined by IAP guidelines and were assigned to the treatment group. They had no history of regular use of NSAIDs, active peptic ulcer, renal dysfunction or allergy to NSAIDs. Administration of sulindac (150 mg twice daily) to the treatment group was continued for 18 months. This dosage was chosen according to the previous chemopreventive studies for colorectal cancer [14, 15]. To prevent mucosal damage by sulindac, omeprazole (20 mg once daily) was also administered. The remaining 12 patients included 11 patients whose lesions did not meet the criteria for surgical resection and one patient (case 11) who had a history of aspirin asthma and refused surgery, although surgical resection was indicated for her lesion. These 12 patients comprised the control group.

Branch duct diameter and main pancreatic duct diameter were monitored by either MRCP or CT twice (at 6 and 18 months) during the observation period. The height of mural nodules was measured by endoscopic ultrasonography (EUS).

Immunohistochemistry

To explore the putative target molecule for sulindac, we performed immunohistochemical studies of cyclooxygenase-1 (COX-1), cyclooxygenase-2 (COX-2) and glutathione-*S*-transferase π (GST-π) using eight specimens of BD-IPMNs that had been resected at our institution between 2000 and 2007. None were from the treatment or control group. In all cases, not only high-grade lesions but also low-grade lesions spreading to the surrounding areas were evaluated. Lesions corresponding to mucinous hyperplasia according to Soldini et al. [16] were defined as hyperplasia, lesions with low to moderate grade dysplasia according to World Health Organization classification [17, 18] as adenoma and lesions with high grade dysplasia and those with invasive carcinoma, according to World Health Organization classification as carcinoma.

Antigen retrieval was performed in Target Retrieval Solution High pH (DAKO, Carpentaria, CA, USA) heated at 100°C in an autoclave for 5 min. Immunohistochemical staining of COX-1 and COX-2 was performed by the LSAB method using an anti-COX-1 polyclonal antibody (Santa Cruz Biotechnology Inc, Santa Cruz, CA, USA) and anti-COX-2 polyclonal antibody (Santa Cruz Biotechnology

Inc), respectively, and LSAB + System-HRP (DAKO). Immunohistochemical staining of GST-π was performed by the dextran polymer method using an anti-GST-π polyclonal antibody (MBL, Nagoya, Japan) and Envision Kit (DAKO), followed by coloring with 3,3′-diaminobenzidine tetrahydrochloride (DAB) (Wako, Osaka, Japan) and nuclear staining with Gill's hematoxylin solution (Wako). Staining intensity and width of staining area under three microscopic fields with a magnification of 200 × were graded according to the method of Gong et al. [19]. Score of intensity and score of area were multiplied and the resultant number was expressed as shown in Fig. 7.

Statistical analysis

Statistical analyses were performed using the Fisher exact test for gender and multiplicity of lesions and Mann–Whitney U test for age, branch duct diameter, main pancreatic duct diameter and mural nodule height. Spearman's rank correlation coefficient was determined for the relation between the branch duct diameter and mural nodule height. Friedman's test and Wilcoxon signed-rank test were performed to determine changes during the observation period. Differences were considered significant at a P value of less than 0.05 in the above analysis. Wilcoxon signed-rank test was used for multiple comparisons of scores of immunohistochemical staining intensity, and the Bonferroni correction was applied.

Results

Demographics of patients

Demographics of patients and their BD-IPMN lesion on images are shown in Table 1. Although there were no differences in age ($P = 0.39$), gender ($P = 0.37$), multiplicity of lesions ($P = 0.59$), branch duct diameter ($P = 0.12$) and main pancreatic duct diameter ($P = 0.34$) between the treatment and control groups, mural nodule height differed significantly between the two groups ($P = 0.003$). Cases 1–10 comprised the treatment group and cases 11–22 the control group.

In case 1, two dilated branch ducts with diameters of 56 and 24 mm, respectively, were detected by MRCP. A mural nodule was associated with the latter duct. In cases 2, 3, and 4, branch duct diameter exceeded 30 mm and mural nodules were detected. Although the branch duct diameter in cases 5, 6, 8, 9, and 10 was within 30 mm, mural nodules were detected in each of these cases. Case 7 experienced continuous epigastric abdominal pain, which is one of the IAP criteria for surgical resection of the lesion. Thus all patients in the treatment group were recommended to undergo surgery according to IAP guidelines, but rejected the recommendation. Cases 8 and 10 transiently complained of lower abdominal pain, which was irrelevant to the pancreatic lesion.

In the control group, case 11 had a lesion with a branch duct diameter >30 mm, main pancreatic duct diameter >6 mm, and mural nodule, which undoubtedly met the criteria of surgical resection, but she rejected operation. This patient had a history of aspirin asthma and therefore was not eligible for treatment with sulindac. The remaining 11 patients in the control group had lesions that did not indicate surgical resection.

To evaluate the relation between branch duct diameter and mural nodule height as determined by either MRCP or CT and EUS, respectively, we conducted Spearman rank-order correlation coefficient analysis and found no statistically significant correlation ($r = 0.40$, $P = 0.067$).

Changes in branch duct diameter in the treatment group and control group during the 18-month observation period

In the treatment group, there was an apparent decrease in branch duct diameter during the period of treatment in cases 1, 2, 3, 4, 8, and 10, although regrowth of the diameter of the branch duct after 6 months was observed in Patient 2. On the other hand, in cases 5, 6, 7, and 9, the branch duct diameter was unchanged. However, when the Friedman test was applied to this treatment group as a whole, the decrease in branch duct diameter was statistically significant ($P = 0.000055$). In the control group, the branch duct diameter tended to increase although the increment was not statistically significant ($P = 0.12$). Of note, in case 16, the branch duct diameter transiently increased at month 6 and decreased at month 18, possibly reflecting a change in the balance between the rate of mucin production by the mural nodule and the drainage rate of mucin fluid from the branch duct (Fig. 1.).

Changes in diameter of the main pancreatic duct in the treatment and control groups during the 18-month observation period

There were no significant changes in the diameter of the main pancreatic duct in both the treatment and control groups, including case 11, whose MPD was apparently dilated (Fig. 2.).

Changes in mural nodule height in the treatment and control groups during the 18-month observation period

In the entire treatment group, with the exception of cases 4 and 7 who had no mural nodules, mural nodule height

Table 1 Demographics of patients and their BD-IPMN lesions on images

	Case number	Age	Gender	Number of lesions	Location of main lesion	Indication of resection (reason for not undergoing operation)	Symptom at the diagnosis	Imaging modalities	Branch duct diameter (mm)	Main pancreatic duct diameter (mm)	Mural nodule height (mm)
Treatment group	1	55	M	2	Head	Yes (rejected)	Asymptomatic	MR + EUS	56 (24)[a]	5	0 (5)[a]
	2	78	M	1	Head	Yes (rejected)	Transient abdominal pain	CT + EUS	42	6	6
	3	74	F	1	Head	Yes (rejected)	Asymptomatic	MR + EUS	36	1	3
	4	65	M	1	Head	Yes (rejected)	Asymptomatic	MR + EUS	33	3	0
	5	70	M	3	Head	Yes (rejected)	Asymptomatic	MR + EUS	26	3	1
	6	47	M	1	Body	Yes (rejected)	Asymptomatic	CT + EUS	20	0	3
	7	61	F	1	Body	Yes (rejected)	Continuous abdominal pain	CT + EUS	17	3	0
	8	57	F	1	Head	Yes (rejected)	Transient abdominal pain	CT + EUS	17	2	7
	9	63	M	1	Tail	Yes (rejected)	Asymptomatic	MR + EUS	16	4	3
	10	57	F	Multiple	Head	Yes (rejected)	Asymptomatic	MR + EUS	13	2	4
Median		63.0							23.0	3.0	3.0
Control group	11	78	F	1	Body	Yes (asthma)	Asymptomatic	CT + EUS	40	15	7
	12	47	M	1	Head	No	Asymptomatic	MR + EUS	29	4	0
	13	86	F	2	Head	No	Asymptomatic	MR + EUS	23	0	0
	14	75	F	3	Head	No	Asymptomatic	MR + EUS	20	4	0
	15	62	M	1	Body	No	Asymptomatic	CT + EUS	19	0	0
	16	85	M	1	Body	No	Asymptomatic	MR + EUS	17	2	0
	17	62	F	1	Head	No	Asymptomatic	CT + EUS	17	0	0
	18	60	F	1	Body	No	Transient abdominal pain	MR + EUS	17	0	0
	19	57	F	Multiple	Tail	No	Asymptomatic	CT + EUS	15	2	0
	20	57	M	1	Head	No	Transient abdominal pain	MR + EUS	14	2	0
	21	72	F	2	Body	No	Asymptomatic	MR + EUS	11	4	0
	22	65	F	Multiple	Head	No	Asymptomatic	MR + EUS	10	3	0
Median		63.5							17.0	2.0	0

[a] Number in parentheses indicates branch duct diameter and mural nodule height of the smaller lesion